

Quantum Ensemble Classification: A Sampling-based Learning Control Approach

Chunlin Chen, Daoyi Dong, Bo Qi, Ian R. Petersen, Herschel Rabitz

Abstract

Quantum ensemble classification has significant applications in discrimination of atoms (or molecules), separation of isotopic molecules and quantum information extraction. However, quantum mechanics forbids deterministic discrimination among nonorthogonal states. The classification of inhomogeneous quantum ensembles is very challenging since there exist variations in the parameters characterizing the members within different classes. In this paper, we recast quantum ensemble classification as a supervised quantum learning problem. A systematic classification methodology is presented by using a sampling-based learning control (SLC) approach for quantum discrimination. The classification task is accomplished via simultaneously steering members belonging to different classes to their corresponding target states (e.g., mutually orthogonal states). Firstly a new discrimination method is proposed for two similar quantum systems. Then an SLC method is presented for quantum ensemble classification. Numerical results demonstrate the effectiveness of the proposed approach for the binary classification of two-level quantum ensembles and the multiclass classification of multilevel quantum ensembles.

Index Terms

This work was supported by the Natural Science Foundation of China (Nos.61273327 and 61004049), by the Australian Research Council (DP130101658 and FL110100020) and by the US NSF (No. CHE-0718610).

C. Chen is with the Department of Control and System Engineering, Nanjing University, Nanjing 210093, China and with the Department of Chemistry, Princeton University, Princeton, New Jersey 08544, USA (email: clchen@nju.edu.cn).

D. Dong is with the School of Engineering and Information Technology, University of New South Wales at the Australian Defence Force Academy, Canberra, ACT 2600, Australia (email: daoyidong@gmail.com).

B. Qi is with the Key Laboratory of Systems and Control, Academy of Mathematics and Systems Science, Chinese Academy of Sciences, Beijing 100190, China (email: qibo@amss.ac.cn).

I. R. Petersen is with the School of Engineering and Information Technology, University of New South Wales at the Australian Defence Force Academy, Canberra, ACT 2600, Australia (email: i.r.petersen@gmail.com).

H. Rabitz is with the Department of Chemistry, Princeton University, Princeton, New Jersey 08544, USA (email: hrabitz@princeton.edu).

Quantum ensemble classification (QEC), quantum discrimination, inhomogeneous ensembles, sampling-based learning control (SLC).

I. INTRODUCTION

Optimal discrimination [1], [2] and classification [3] of quantum states or quantum systems is a central topic in quantum information technology [4]. This interdisciplinary research area involves pattern recognition in machine learning, quantum control in quantum technology [5]-[9] and very common laboratory problems of isolating similar species in chemical physics. In existing research, discrimination of two similar quantum systems (e.g., similar molecules) has been extensively investigated [10]-[21].

Many practical quantum systems exist in the form of quantum ensembles. A quantum ensemble consists of a large number of (e.g., 10^{23}) single quantum systems (e.g., identical spin systems or molecules). Each single quantum system in a quantum ensemble is referred to as a member of the ensemble. Quantum ensembles have wide applications in emerging quantum technology including quantum computation [22], long-distance quantum communication [23], and magnetic resonance imaging [24]. In practical applications, the members of a quantum ensemble could show variations in the parameters that characterize the system dynamics [25], [26]. Such an ensemble is called an inhomogeneous quantum ensemble [27]. For example, the spins of an ensemble in nuclear magnetic resonance (NMR) experiments may have a large dispersion in the strength of the applied radio frequency field (RF inhomogeneity) and their natural frequencies (Larmor dispersion) [26]. In complex systems, there are intrinsic inhomogeneities of even chemically identical molecules due to different conformations and diverse environments [28]. The classification of inhomogeneous quantum ensembles is a significant issue and has great potential applications in the discrimination of atoms (or molecules), the separation of isotopic molecules and quantum information extraction.

However, quantum mechanics forbids deterministic discrimination among nonorthogonal states [1]. A useful idea is to first drive the members of a quantum ensemble from an initial state to different orthogonal states corresponding to different classes (e.g., eigenstates) before classifying them. Usually, it is impractical to employ different control inputs for individual members of a quantum ensemble in physical experiments. Hence, it is important to develop new approaches for designing external control fields that can simultaneously steer the ensemble of inhomogeneous

systems from an initial state to different target states when variations exist in their internal parameters. Some quantum control techniques such as the multidimensional pseudospectral method [24], [29], the Lyapunov control methodology [30] and the sampling-based learning control approach [27] may provide inspiration for the solution to this problem.

In this paper, we recast the quantum ensemble classification task as a supervised quantum learning problem and present a systematic classification methodology by using a sampling-based learning control (SLC) method [27], [31] in quantum discrimination. In this method, we first learn an optimal control strategy to steer the members in a quantum ensemble belonging to different classes into their corresponding target states, and then employ a physical read-out process (e.g., projective measurement, fluorescence images of molecules [28], Stern-Gerlach experiment for spin systems [4], [32]) to classify these classes. For example, the states of single molecules could be read out using a visualization technique, where the highly photostable chromophore dinaphthoquatterylenebis (dicarboximide) (DNQDI) is embedded in thin polymer films in concentrations sufficiently low to allow individual DNQDI molecules to be spatially resolved in an epifluorescence confocal microscope (for details, see [28]). It is feasible to read out the intensity of the single-molecule fluorescence after they are excited with laser pulses. For a spin ensemble, when some members are driven to spin up and the other are driven to spin down, it is feasible to physically separate the two classes of members using Stern-Gerlach experiments [4]. We first develop a new approach for the discrimination of two similar quantum systems and the binary classification of quantum ensembles. Then we apply the proposed approach to multiclass classification of multilevel quantum ensembles.

This paper is organized as follows. Section **II** formulates the learning problem for quantum ensemble classification. A control design method is presented in Section **III** for quantum discrimination of similar quantum systems. In Section **IV** an SLC method is proposed for the binary classification of quantum ensembles and numerical results are demonstrated for an ensemble of two-level spin systems. The proposed approach is applied to the multiclass classification of multi-level quantum ensembles in Section **V**. Conclusions are presented in Section **VI**.

II. PROBLEM FORMULATION

We focus on finite-dimensional closed quantum systems. The state evolution of a quantum system is described by the following Schrödinger equation (setting the reduced Plank constant

$\hbar = 1$:

$$\begin{cases} \frac{d}{dt}|\psi(t)\rangle = -iH(t)|\psi(t)\rangle \\ t \in [0, T], |\psi(0)\rangle = |\psi_0\rangle \end{cases} \quad (1)$$

where $|\psi(t)\rangle$ (quantum state) is a unit complex vector on the underlying Hilbert space, $H(t)$ is the system Hamiltonian and $i = \sqrt{-1}$. The dynamics of the system is governed by a time-dependent Hamiltonian of the form

$$H(t) = H_0 + H_c(t) = H_0 + \sum_{m=1}^M u_m(t)H_m, \quad (2)$$

where H_0 is the free Hamiltonian of the system and $H_c(t) = \sum_{m=1}^M u_m(t)H_m$ is the time-dependent control Hamiltonian that represents the interaction of the system with the external fields $u_m(t)$ (real-valued and square-integrable functions). H_m are Hermitian operators through which the controls couple to the system. The solution of (1) is given by $|\psi(t)\rangle = U(t)|\psi_0\rangle$, where the propagator $U(t)$ satisfies the following equation (I is an identity matrix)

$$\begin{cases} \frac{d}{dt}U(t) = -iH(t)U(t), \\ t \in [0, T], U(0) = I. \end{cases} \quad (3)$$

In this paper, we consider the classification problem for a quantum ensemble of similar members with different Hamiltonians, which is referred to as *quantum ensemble classification* (QEC). Suppose that for an inhomogeneous quantum ensemble, we are given an unknown member belonging to a certain class, how well can we predict the class that the unknown member belongs to? In classical machine learning, this problem can be solved using typical supervised learning algorithms with a training set. However, this problem is much more difficult for quantum systems because we can not achieve deterministic discrimination for given quantum systems unless they lie in mutually orthogonal states. We have to drive the members from different classes to appropriate orthogonal states (e.g., eigenstates) before we can discriminate them with high accuracy. The sampling-based learning control approach presented for the control of inhomogeneous quantum ensembles can be combined with supervised learning for QEC. We define the training set for the QEC problem as follows.

Definition 1 (Training set of QEC): A training set consists of N quantum systems (each of them labeled with an associated class) that are chosen from the quantum ensemble and the set is denoted as

$$D_N = \{(H^1(t), y_1), (H^2(t), y_2), \dots, (H^N(t), y_N)\} \quad (4)$$

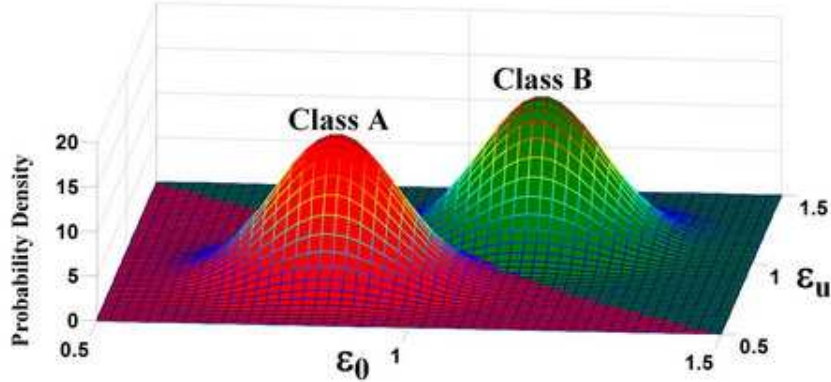


Fig. 1. Example of an inhomogeneous quantum ensemble consisting of two classes (*A* and *B*) with the inhomogeneity parameters having Gaussian distribution.

where $H^n(t)$ ($n = 1, 2, \dots, N$) describes the n th quantum system in the training set and y_n is the associated class that this quantum system belongs to.

For ease of presentation, we first consider an inhomogeneous ensemble consisting of two classes of members (i.e., classes *A* and *B*) and propose an SLC approach for this binary quantum ensemble classification problem using a spin- $\frac{1}{2}$ quantum ensemble example. We further extend the proposed approach to the classification problem with multi classes and multi-level quantum ensembles. For the binary quantum ensemble classification problem, the Hamiltonian of each member has the following form

$$\begin{cases} H_{\varepsilon_0, \varepsilon_u}^A(t) = g_0^A(\varepsilon_0)H_0 + g_u^A(\varepsilon_u) \sum_{m=1}^M u_m(t)H_m \\ H_{\varepsilon_0, \varepsilon_u}^B(t) = g_0^B(\varepsilon_0)H_0 + g_u^B(\varepsilon_u) \sum_{m=1}^M u_m(t)H_m. \end{cases} \quad (5)$$

$g_0^A(\cdot)$ and $g_u^A(\cdot)$ are known functions, while the inhomogeneity parameters ε_0 and ε_u in the Hamiltonian $H_{\varepsilon_0, \varepsilon_u}^A(t)$ for class *A* are characterized by the distribution functions $d_0^A(\varepsilon_0)$ and $d_u^A(\varepsilon_u)$, respectively. We assume that the parameters ε_0 and ε_u are time independent. A similar expression to (5) is defined for the Hamiltonian $H_{\varepsilon_0, \varepsilon_u}^B(t)$ of class *B*.

An example is shown in Fig. 1 to describe the inhomogeneity of the quantum ensemble consisting of two classes of members with parameters in each class having Gaussian distribution. The function $d_0^A(\varepsilon_0)$ ($d_0^B(\varepsilon_0)$) characterizes the distribution of inhomogeneity in the free Hamiltonian for class *A* (*B*) and $d_u^A(\varepsilon_u)$ ($d_u^B(\varepsilon_u)$) characterizes the distribution of inhomogeneity

in the control Hamiltonian for class A (B). Fig. 1 shows a 2D Gaussian distribution case regarding the parameters ε_0 and ε_u .

For a binary quantum ensemble classification task, the objective is to design a control strategy $u(t) = \{u_m(t), m = 1, 2, \dots, M\}$ to simultaneously stabilize the members in class A (with different ε_0 and ε_u) from an initial state $|\psi_0\rangle$ to the same target state $|\psi_{\text{target}A}\rangle$, and at the same time to stabilize the members in class B (with different ε_0 and ε_u) from $|\psi_0\rangle$ to another target state $|\psi_{\text{target}B}\rangle$. A binary QEC problem can be described by the following definition.

Definition 2 (Binary QEC): A binary quantum ensemble classification (binary QEC) task is to construct a binary quantum classifier to maximize the classification accuracy, where this binary quantum classifier consists of three steps:

- 1) *Training step:* Learn an optimal control strategy $u(t)$ with the training set

$$D_N = \{(H^1(t), y_1), (H^2(t), y_2), \dots, (H^N(t), y_N)\},$$

where $y_n \in \{A, B\}$ (A and B are symbolic constants) and $H^n(t)$ ($n = 1, 2, \dots, N$) is the time-dependent Hamiltonian describing the n th member in the training set.

- 2) *Coherent control step:* Apply the learned optimal control strategy $u(t)$ to all the members of the quantum ensemble.
- 3) *Classification step:* Predict the class y_j of an unknown quantum system in the quantum ensemble using a corresponding physical read-out process, where $j = 1, 2, \dots, N_e$ and N_e is the number of members in the quantum ensemble.

For example, a schematic of the classification process for a spin- $\frac{1}{2}$ quantum ensemble is demonstrated in Fig. 2. As shown in Fig. 2, an ensemble of inhomogeneous spin- $\frac{1}{2}$ systems is prepared with an initial state. After learning using a training set from the quantum ensemble, we can find an optimal control strategy to simultaneously drive all the members of class A to the target state (spin up) and all the members of class B to another target state (spin down). Then we can use a Stern-Gerlach experiment to physically separate the two classes.

From Definition 2 it is clear that the key task of the classification problem is to learn an optimal control strategy in the training step for the binary quantum classifier. The training performance is described by a *performance function* $J(u)$ for each learned control strategy $u = \{u_m(t), m = 1, 2, \dots, M\}$. The binary QEC problem can then be formulated as a maximization problem as

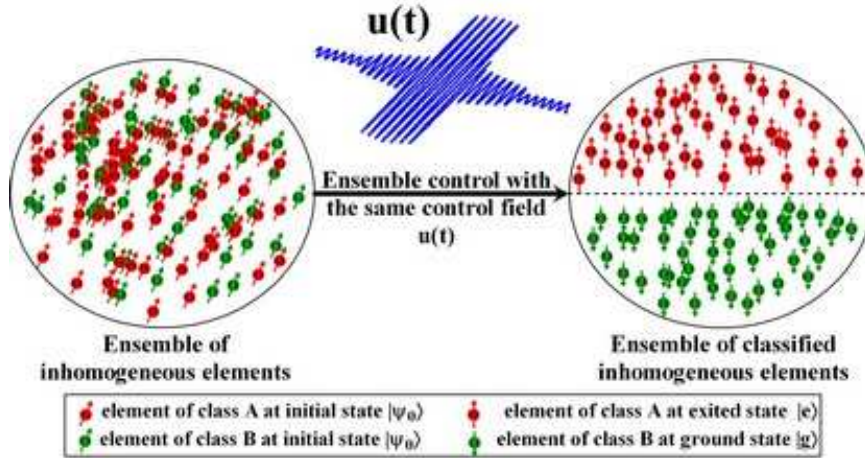


Fig. 2. Schematic of the binary classification for a spin- $\frac{1}{2}$ quantum ensemble.

follows:

$$\begin{aligned}
 \max_u J(u) &:= \max_u \{w_A \mathbb{E}[J_{\varepsilon_0, \varepsilon_u}^A(u)] + w_B \mathbb{E}[J_{\varepsilon_0, \varepsilon_u}^B(u)]\} \\
 \text{s.t. } t &\in [0, T] \\
 |\psi_{\varepsilon_0, \varepsilon_u}^A(0)\rangle &= |\psi_{\varepsilon_0, \varepsilon_u}^B(0)\rangle = |\psi_0\rangle \\
 \left\{ \begin{array}{l} \frac{d}{dt} |\psi_{\varepsilon_0, \varepsilon_u}^A(t)\rangle = -iH_{\varepsilon_0, \varepsilon_u}^A(t) |\psi_{\varepsilon_0, \varepsilon_u}^A(t)\rangle \\ H_{\varepsilon_0, \varepsilon_u}^A(t) = g_0^A(\varepsilon_0)H_0 + g_u^A(\varepsilon_u) \sum_{m=1}^M u_m(t)H_m \end{array} \right. & (6) \\
 J_{\varepsilon_0, \varepsilon_u}^A(u) &:= |\langle \psi_{\varepsilon_0, \varepsilon_u}^A(T) | \psi_{\text{targetA}} \rangle|^2 \\
 \left\{ \begin{array}{l} \frac{d}{dt} |\psi_{\varepsilon_0, \varepsilon_u}^B(t)\rangle = -iH_{\varepsilon_0, \varepsilon_u}^B(t) |\psi_{\varepsilon_0, \varepsilon_u}^B(t)\rangle \\ H_{\varepsilon_0, \varepsilon_u}^B(t) = g_0^B(\varepsilon_0)H_0 + g_u^B(\varepsilon_u) \sum_{m=1}^M u_m(t)H_m \end{array} \right. \\
 J_{\varepsilon_0, \varepsilon_u}^B(u) &:= |\langle \psi_{\varepsilon_0, \varepsilon_u}^B(T) | \psi_{\text{targetB}} \rangle|^2
 \end{aligned}$$

where $w_A, w_B \in [0, 1]$ are the weights assigned to classes A and B , respectively, satisfying $w_A + w_B = 1$. $J_{\varepsilon_0, \varepsilon_u}^A(u)$ is a measure of classification accuracy for each member in class A regarding the target state $|\psi_{\text{targetA}}\rangle$ and $\mathbb{E}[J_{\varepsilon_0, \varepsilon_u}^A(u)]$ denotes the average value of $J_{\varepsilon_0, \varepsilon_u}^A(u)$ over class A . A similar expression holds for class B . It is clear that $J_{\varepsilon_0, \varepsilon_u}^A$ and $J_{\varepsilon_0, \varepsilon_u}^B$ depend implicitly on the control strategy $u(t)$ through the Schrödinger equation. The performance $J(u)$ represents the weighted accuracy of classification.

III. DISCRIMINATION OF TWO SIMILAR QUANTUM SYSTEMS

Optimal dynamic discrimination between two similar quantum systems has been investigated using different techniques [2], [10]. The quantum discrimination problem can be taken as a special case of the binary QEC problem with the number of members in an ensemble $N_e = 2$. In this sense, control design for quantum discrimination is the foundation of quantum ensemble classification. In this section, we develop a gradient-based learning control method for quantum discrimination of two similar quantum systems and then we extend the method to control design for binary QEC in Section IV.

A. Learning control design for quantum discrimination

Suppose two similar quantum systems to be discriminated a and b have the following Hamiltonians:

$$\begin{cases} H_{\varepsilon_0^a, \varepsilon_u^a}^a(t) = g_0(\varepsilon_0^a)H_0 + g_u(\varepsilon_u^a) \sum_{m=1}^M u_m(t)H_m \\ H_{\varepsilon_0^b, \varepsilon_u^b}^b(t) = g_0(\varepsilon_0^b)H_0 + g_u(\varepsilon_u^b) \sum_{m=1}^M u_m(t)H_m \end{cases} \quad (7)$$

where ε_0^a , ε_u^a , ε_0^b and ε_u^b are predefined constants for functions $g_0(\cdot)$ and $g_u(\cdot)$. a and b are prepared in the same initial state $|\psi_0\rangle$. The objective is to find an optimal control strategy $u(t)$ ($t \in [0, T]$) to drive the state of system a to the target state $|\psi_{\text{targetA}}\rangle$ and the state of system b to the target state $|\psi_{\text{targetB}}\rangle$ at the same time. Usually, we let $\langle \psi_{\text{targetA}} | \psi_{\text{targetB}} \rangle = 0$ so that we can completely discriminate system a from system b . The control performance $J(u)$ is redefined for the discrimination problem as

$$J(u) := w_a J_{\varepsilon_0^a, \varepsilon_u^a}^a(u) + w_b J_{\varepsilon_0^b, \varepsilon_u^b}^b(u) \quad (8)$$

where $w_a, w_b \in [0, 1]$ are the weights assigned to the associated systems, respectively, and

$$\begin{aligned} J_{\varepsilon_0^a, \varepsilon_u^a}^a(u) &:= |\langle \psi_{\varepsilon_0^a, \varepsilon_u^a}^a(T) | \psi_{\text{targetA}} \rangle|^2, \\ J_{\varepsilon_0^b, \varepsilon_u^b}^b(u) &:= |\langle \psi_{\varepsilon_0^b, \varepsilon_u^b}^b(T) | \psi_{\text{targetB}} \rangle|^2. \end{aligned} \quad (9)$$

Here we set $w_a = w_b = 0.5$ for the discrimination problem.

In order to find an optimal control strategy $u^* = \{u_m^*(t), (t \in [0, T]), m = 1, 2, \dots, M\}$ for the discrimination problem, it is a good choice to follow the direction of the gradient of $J(u)$ as an ascent direction. For ease of notation, we present the method for $M = 1$. We introduce a

time-like variable s to characterize different control strategies $u^{(s)}(t)$. Then a gradient flow in the control space can be defined as

$$\frac{du^{(s)}}{ds} = \nabla J(u^{(s)}), \quad (10)$$

where $\nabla J(u)$ denotes the gradient of $J(u)$ with respect to the control u . It is easy to show that if $u^{(s)}$ is the solution of (10) starting from an arbitrary initial condition $u^{(0)}$, then the value of $J(u)$ is increasing along $u^{(s)}$, i.e., $\frac{d}{ds}J(u^{(s)}) \geq 0$. In other words, starting from an initial guess u^0 , we solve the following initial value problem

$$\begin{cases} \frac{du^{(s)}}{ds} = \nabla J(u^{(s)}) = w_a \nabla J_{\varepsilon_0^a, \varepsilon_u^a}^a(u^{(s)}) + w_b \nabla J_{\varepsilon_0^b, \varepsilon_u^b}^b(u^{(s)}) \\ u^{(0)} = u^0 \end{cases} \quad (11)$$

in order to find a control strategy which maximizes $J(u)$. This initial value problem can then be solved numerically by a forward Euler method (or other high order integration methods) over the s -domain, i.e.,

$$u(s + \Delta s, t) = u(s, t) + \Delta s \nabla J(u^{(s)}). \quad (12)$$

As for practical applications, we present its iterative approximation version to find the optimal control $u^*(t)$, where we use k as an index of iterations instead of the variable s and denote the control at iteration step k as $u^k(t)$. Equation (12) can be rewritten as

$$u^{k+1}(t) = u^k(t) + \eta_k \nabla J(u^k), \quad (13)$$

where η_k is the updating step (learning rate) for the k th iteration and

$$\nabla J(u^k) = w_a \nabla J_{\varepsilon_0^a, \varepsilon_u^a}^a(u^k) + w_b \nabla J_{\varepsilon_0^b, \varepsilon_u^b}^b(u^k). \quad (14)$$

In addition, we have the gradient of $J_{\varepsilon_0^a, \varepsilon_u^a}^a(u^k)$ with respect to the control u as follows (a detailed derivation is provided in the appendix)

$$\nabla J_{\varepsilon_0^a, \varepsilon_u^a}^a(u^k) = 2\Im \left(\langle \psi_{\varepsilon_0^a, \varepsilon_u^a}^a(T) | \psi_{\text{targetA}} \rangle \langle \psi_{\text{targetA}} | G_1^a(t) | \psi_0 \rangle \right), \quad (15)$$

where $\Im(\cdot)$ denotes the imaginary part of a complex number, $G_1^a(t) = U_{\varepsilon_0^a, \varepsilon_u^a}(T) U_{\varepsilon_0^a, \varepsilon_u^a}^\dagger(t) g_u(\varepsilon_u^a) H_1 U_{\varepsilon_0^a, \varepsilon_u^a}(t)$, and the propagator $U_{\varepsilon_0^a, \varepsilon_u^a}(t)$ satisfies

$$\frac{d}{dt} U_{\varepsilon_0^a, \varepsilon_u^a}(t) = -i H_{\varepsilon_0^a, \varepsilon_u^a}^a(t) U_{\varepsilon_0^a, \varepsilon_u^a}(t), \quad U(0) = I.$$

A similar expression can also be derived for $\nabla J_{\varepsilon_0^b, \varepsilon_u^b}^b(u^k)$. When we generalize the gradient flow method to the case with $M > 1$, for each control $u_m(t)$ ($m = 1, 2, \dots, M$) of the control strategy $u(t)$, we have

$$\begin{aligned} \nabla J(u_m^k) = & 2w_a \Im \left(\langle \psi_{\varepsilon_0^a, \varepsilon_u^a}^a(T) | \psi_{\text{targetA}} \rangle \langle \psi_{\text{targetA}} | G_m^a(t) | \psi_0 \rangle \right) \\ & + 2w_b \Im \left(\langle \psi_{\varepsilon_0^b, \varepsilon_u^b}^b(T) | \psi_{\text{targetB}} \rangle \langle \psi_{\text{targetB}} | G_m^b(t) | \psi_0 \rangle \right) \end{aligned} \quad (16)$$

where

$$\begin{aligned} G_m^a(t) &= U_{\varepsilon_0^a, \varepsilon_u^a}(T) U_{\varepsilon_0^a, \varepsilon_u^a}^\dagger(t) g_u(\varepsilon_u^a) H_m U_{\varepsilon_0^a, \varepsilon_u^a}(t), \\ G_m^b(t) &= U_{\varepsilon_0^b, \varepsilon_u^b}(T) U_{\varepsilon_0^b, \varepsilon_u^b}^\dagger(t) g_u(\varepsilon_u^b) H_m U_{\varepsilon_0^b, \varepsilon_u^b}(t). \end{aligned}$$

A gradient flow based iterative learning algorithm for the discrimination of quantum systems is shown in *Algorithm 1*.

Algorithm 1. Gradient flow based iterative learning for quantum discrimination

- 1: Set the index of iterations $k = 0$
- 2: Choose a set of arbitrary controls $u^{k=0}(t) = \{u_m^0(t), m = 1, 2, \dots, M\}, t \in [0, T]$
- 3: **repeat** (for each iterative process)
- 4: Compute the propagator $U_{\varepsilon_0^a, \varepsilon_u^a}^k(t)$ and $U_{\varepsilon_0^b, \varepsilon_u^b}^k(t)$ for systems a and b , respectively, with the control strategy $u^k(t)$
- 5: **repeat** (for each control $u_m(t)$ ($m = 1, 2, \dots, M$) of the control vector $u^k(t)$)
- 6: $\delta_m^k(t) := \nabla J(u_m^k)$ and compute $\nabla J(u_m^k)$ using equation (16)
- 7: $u_m^{k+1}(t) = u_m^k(t) + \eta_k \delta_m^k(t)$
- 8: **until** $m = M$
- 9: $k = k + 1$
- 10: **until** the learning process ends
- 11: The optimal control strategy $u^*(t) = \{u_m^*(t)\} = \{u_m^k(t)\}, m = 1, 2, \dots, M$

Remark 1: The numerical solution of control design using *Algorithm 1* is always difficult with a time varying continuous control strategy $u(t)$. In the practical implementation, we usually divide the time duration $[0, T]$ equally into a number of time slices Δt and assume that the controls are constant within each time slice. Instead of $t \in [0, T]$, the time index is $t_q = qT/Q$, where $Q = T/\Delta t$ and $q = 1, 2, \dots, Q$.

B. Numerical examples

To demonstrate this learning control method for discrimination of two similar quantum systems, we consider two-level (spin- $\frac{1}{2}$) systems. We denote the Pauli matrices $\sigma = (\sigma_x, \sigma_y, \sigma_z)$ as follows:

$$\sigma_x = \begin{pmatrix} 0 & 1 \\ 1 & 0 \end{pmatrix}, \quad \sigma_y = \begin{pmatrix} 0 & -i \\ i & 0 \end{pmatrix}, \quad \sigma_z = \begin{pmatrix} 1 & 0 \\ 0 & -1 \end{pmatrix}. \quad (17)$$

For a two-level quantum system, we may assume the free Hamiltonian $H_0 = \frac{1}{2}\sigma_z$. Its two eigenstates are denoted as $|0\rangle$ (e.g., spin up) and $|1\rangle$ (e.g., spin down). To control a two-level quantum system, we use the control Hamiltonian of $H_u = \frac{1}{2}u_1(t)\sigma_x + \frac{1}{2}u_2(t)\sigma_y$. Hence,

$$H(t) = H_0 + H_u(t) = \frac{1}{2}\sigma_z + \frac{1}{2}u_1(t)\sigma_x + \frac{1}{2}u_2(t)\sigma_y. \quad (18)$$

For two similar spin- $\frac{1}{2}$ systems, the Hamiltonian of each system can be described as

$$\begin{aligned} H_{\varepsilon_0, \varepsilon_u}(t) &= g_0(\varepsilon_0)H_0 + g_u(\varepsilon_u)H_u(t) \\ &= \frac{1}{2}g_0(\varepsilon_0)\sigma_z + \frac{1}{2}g_u(\varepsilon_u)(u_1(t)\sigma_x + u_2(t)\sigma_y). \end{aligned} \quad (19)$$

We assume $g_0(\varepsilon_0) = \varepsilon_0$ and $g_u(\varepsilon_u) = \varepsilon_u$. The state of the two quantum systems can be represented in the eigen-basis of H_0 by $|\psi(t)\rangle = c_0(t)|0\rangle + c_1(t)|1\rangle$. Denote $C(t) = (c_0(t), c_1(t))^T$, where $c_0(t)$ and $c_1(t)$ are complex numbers, and x^T represents the transpose of x . We have

$$\begin{pmatrix} \dot{c}_0(t) \\ \dot{c}_1(t) \end{pmatrix} = \begin{pmatrix} 0.5\varepsilon_0 i & \varepsilon_u f(u) \\ -\varepsilon_u f^*(u) & -0.5\varepsilon_0 i \end{pmatrix} \begin{pmatrix} c_0(t) \\ c_1(t) \end{pmatrix}, \quad (20)$$

where $f(u) = u_2(t) - 0.5iu_1(t)$, $(\varepsilon_0, \varepsilon_u) = (\varepsilon_0^a, \varepsilon_u^a)$ for system a and $(\varepsilon_0, \varepsilon_u) = (\varepsilon_0^b, \varepsilon_u^b)$ for system b .

Define the performance function as

$$\begin{aligned} J(u) &= \frac{1}{2}J^a(u) + \frac{1}{2}J^b(u) \\ &= \frac{1}{2}|\langle C_a(T)|C_{\text{targetA}}\rangle|^2 + \frac{1}{2}|\langle C_b(T)|C_{\text{targetB}}\rangle|^2. \end{aligned} \quad (21)$$

The task is to find a control $u(t)$ to maximize the performance function in (21). For a given small threshold $\varepsilon > 0$, if $|J(u^{k+1}) - J(u^k)| < \varepsilon$ for uninterrupted n_e steps, we may think we find a suitable control law for the problem. In this paper, we set $\varepsilon = 10^{-4}$ and $n_e = 100$ in all numerical experiments.

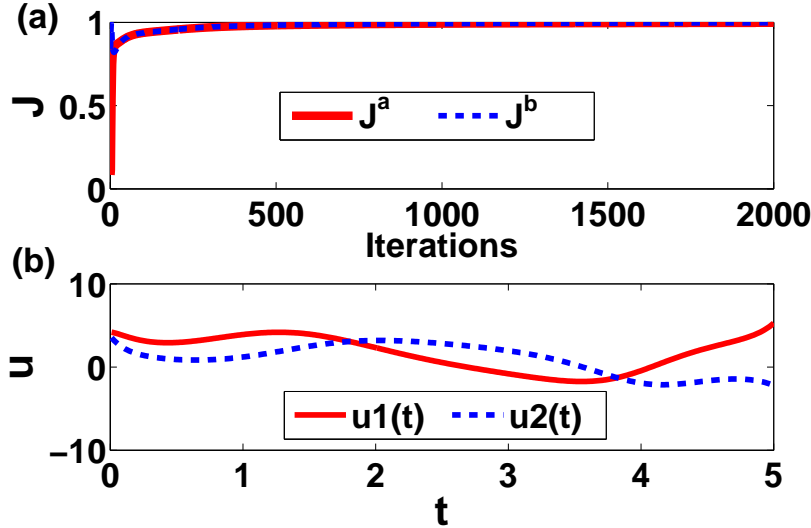


Fig. 3. Learning performance of discrimination between system a ($(\varepsilon_0^a, \varepsilon_u^a) = (0.9, 0.9)$) and system b ($(\varepsilon_0^b, \varepsilon_u^b) = (1.1, 1.1)$). (a) Evolution of performance functions $J^a(u)$ and $J^b(u)$; (b) The learned optimal control strategy $u(t)$.

Now we employ *Algorithm 1* to find the optimal control strategy $u^*(t) = \{u_m^*(t), m = 1, 2\}$ and then apply the optimal control strategy for discriminating system a from system b . The parameter settings are listed as follows: the initial state $C_0 = (1, 0)^T$, i.e., $|\psi_0\rangle = |0\rangle$, and the target state for system a $C_{\text{targetA}} = (1, 0)^T$, i.e., $|\psi_{\text{targetA}}\rangle = |0\rangle$; the target state for system b $C_{\text{targetB}} = (0, 1)^T$, i.e., $|\psi_{\text{targetB}}\rangle = |1\rangle$; The ending time $T = 5$ (in atomic units) and the total time duration $[0, T]$ is equally discretized into $Q = 500$ time slices with each time slice $\Delta t = (t_q - t_{q-1})|_{q=1,2,\dots,Q} = T/Q = 0.01$; the learning rate $\eta_k = 0.2$; the control strategy is initialized as $u^{k=0}(t) = \{u_1^0(t) = \sin t, u_2^0(t) = \sin t\}$.

In the first example, two similar systems a and b are characterized with parameters $(\varepsilon_0^a, \varepsilon_u^a) = (0.9, 0.9)$ and $(\varepsilon_0^b, \varepsilon_u^b) = (1.1, 1.1)$, respectively. The numerical results are shown in Figs. 3-5. As shown in Fig. 3(a), the learning process converges very quickly and the performance function $J(u)$ converges to 0.999 after about 2000 steps of iterative learning with an optimized control strategy $u(t) = \{u_1(t), u_2(t)\}$ in Fig. 3(b). Then we apply the learned optimal control strategy to systems a and b . The evolution of their states can be clearly demonstrated regarding their populations at the state $|0\rangle$ as shown in Fig. 4. At time $t = T = 5$, $|c_0^a(T)|^2 = 1.0000$ and $|c_0^b(T)|^2 = 0.0000$, which indicates that, after the coherent control step, we can discriminate system a from system b using a projective measurement and the success probability is almost

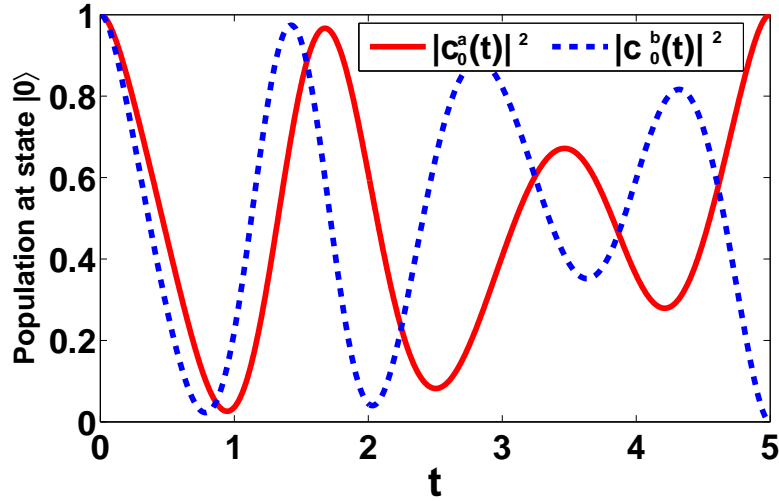


Fig. 4. Evolution of the states of system a ($(\varepsilon_0^a, \varepsilon_u^a) = (0.9, 0.9)$) and system b ($(\varepsilon_0^b, \varepsilon_u^b) = (1.1, 1.1)$) regarding their populations ($|c_0^a(t)|^2$ and $|c_0^b(t)|^2$) at the state $|0\rangle$, respectively.

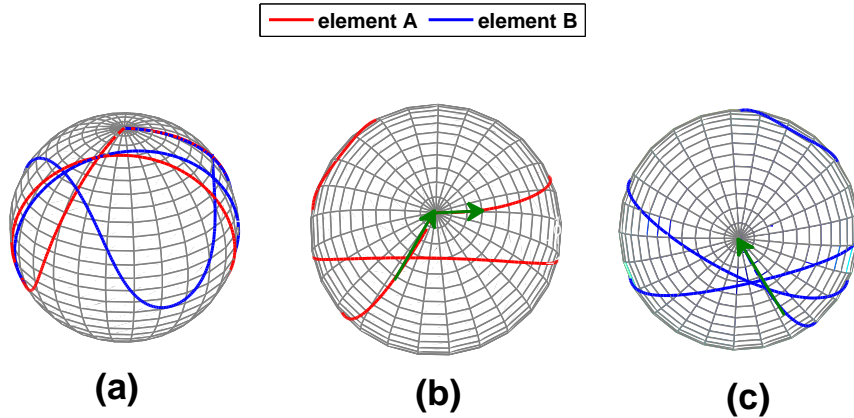


Fig. 5. Demonstration of the state transition trajectories of system a ($(\varepsilon_0^a, \varepsilon_u^a) = (0.9, 0.9)$) and system b ($(\varepsilon_0^b, \varepsilon_u^b) = (1.1, 1.1)$) on the Bloch sphere.

100%.

A 3-D visualized demonstration is further shown in Fig. 5 for the state transition trajectories of systems a and b on the Bloch sphere. For a two-level system, its state can also be represented using a Bloch vector $\mathbf{r} = (x, y, z)$ where $x = \text{tr}\{|\psi\rangle\langle\psi|\sigma_x\}$, $y = \text{tr}\{|\psi\rangle\langle\psi|\sigma_y\}$, $z = \text{tr}\{|\psi\rangle\langle\psi|\sigma_z\}$ and $\text{tr}(\cdot)$ is the trace operator. As shown in Fig. 5, using the same learned control strategy, the state trajectories of systems a and b are successfully driven from the same initial state

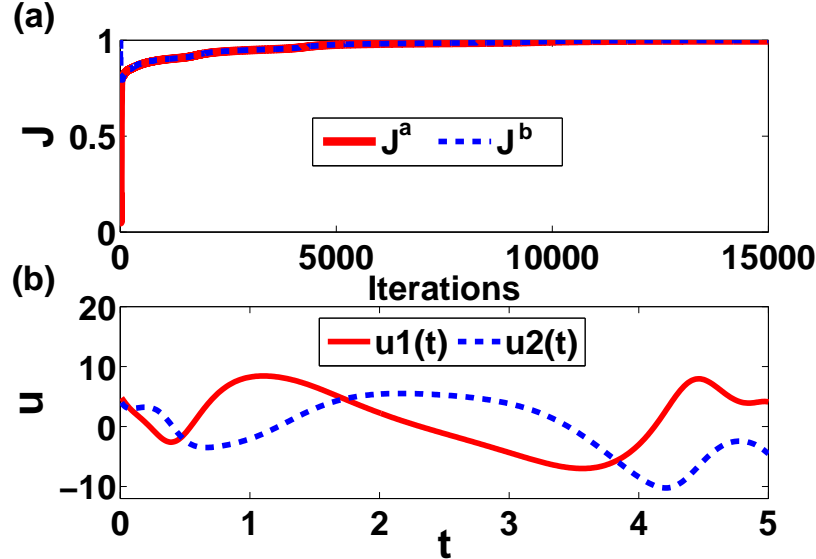


Fig. 6. Learning performance of discrimination between system a ($(\varepsilon_0^a, \varepsilon_u^a) = (0.95, 0.95)$) and system b ($(\varepsilon_0^b, \varepsilon_u^b) = (1.05, 1.05)$). (a) Evolution of performance functions $J^a(u)$ and $J^b(u)$; (b) The learned optimal control strategy $u(t)$.

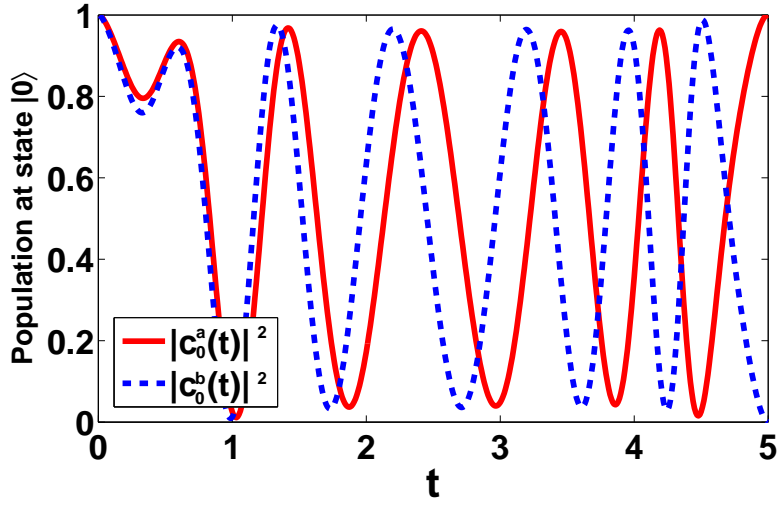


Fig. 7. Evolution of the states of system a ($(\varepsilon_0^a, \varepsilon_u^a) = (0.95, 0.95)$) and system b ($(\varepsilon_0^b, \varepsilon_u^b) = (1.05, 1.05)$) regarding the population at the state $|0\rangle$, respectively.

$|\psi_0\rangle = |0\rangle$ (i.e., $r_0 = (0, 0, 1)$) to different target states of $|\psi_{\text{targetA}}\rangle = |0\rangle$ (i.e., $r_{\text{targetA}} = (0, 0, 1)$) and $|\psi_{\text{targetB}}\rangle = |1\rangle$ (i.e., $r_{\text{targetB}} = (0, 0, -1)$), respectively.

In the second example, two similar systems a and b are characterized with parameters $(\varepsilon_0^a, \varepsilon_u^a) = (0.95, 0.95)$ and $(\varepsilon_0^b, \varepsilon_u^b) = (1.05, 1.05)$. The numerical results are shown in Fig. 6 and Fig. 7. Similar to the first example, we can also successfully learn an optimal control strategy (Fig. 6(b))

to drive systems a and b to different target eigenstates from the same initial state. The evolution of their states is shown in Fig. 7 regarding their populations at the state $|0\rangle$, respectively. By comparing the second example with the first one, it is clear that the difference lies in the similarity between Hamiltonians. For the second example, the increasing of the similarity of Hamiltonians makes it more difficult to discriminate system a from system b . More learning steps (about 15000 steps) are needed for the second example than the first one (around 2000 steps). A larger control strength is also needed for the second example than that in the first one (i.e., the amplitudes of controls in Fig. 6(b) are larger than those in Fig. 3(b)). This phenomenon is comprehensively tested through further numerical experiments with varied parameters. All of the results show that the gradient flow based iterative learning method is successful for discrimination of similar quantum systems and also support the previous findings that optimal dynamic discrimination is feasible for many similar quantum systems in physics and chemistry communities [2], [10]-[16].

IV. QUANTUM ENSEMBLE CLASSIFICATION VIA SLC

Binary classification is to classify the members of a given set of objects into two classes on the basis of whether they have certain properties or not. As introduced in Definition 2, for a binary QEC problem, we have to learn from a training set as defined in Definition 1 and find out an optimal control strategy for all the members in the quantum ensemble. In this section, we combine a sampling-based learning control (SLC) approach into the quantum discrimination method introduced above to solve the QEC problem (i.e., the maximization problem formulated as Equation (6)).

A. SLC for quantum ensemble classification

The first key issue for QEC is how to obtain the training set. Generally there are two ways to construct a training set for QEC: (i) the data is provided initially and the training set can be constructed directly, but we do not know the distribution of parameters that characterize the members belonging to different classes; (ii) no initial training data is provided but we know the distribution of parameters and we can choose samples using the distribution information. The first way is very common in classical machine learning problems, while the second way is more suitable for the classification of quantum systems. In the quantum domain, it is difficult to obtain a specific description for a single system in a quantum ensemble, while we can characterize

an ensemble of similar systems with a distribution of parameters (e.g., Gaussian distribution, Boltzmann distribution and uniform distribution). According to the distribution of parameters for a quantum ensemble, we can choose sample members to construct the training set for the learning control design. This approach is referred to as sampling-based learning control (SLC), which originated in [27], [31] as a general framework for optimal control design of inhomogeneous quantum ensembles and robust control design of quantum systems with uncertainties.

In the SLC approach, a generalized system is constructed by sampling members from the inhomogeneous ensemble. In this paper, we adopt the key idea from SLC and solve the supervised quantum learning problem of QEC via constructing a generalized system using the training set.

Suppose we have obtained a training set $D_N = \{(H^n(t), y_n)\}$ ($n = 1, 2, \dots, N$) for the binary QEC problem, where $y_n \in \{A, B\}$ and $H^n(t)$ is the time-dependent Hamiltonian that describes the n th member of the quantum ensemble. Now we split D_N into two subsets according to the value of y_n and rewrite the training set as follows

$$\begin{aligned} D_N &= D_{N_A} \cup D_{N_B}, \quad N = N_A + N_B, \\ D_{N_A} &= \{(H_{\varepsilon_0^{n_A}, \varepsilon_u^{n_A}}^A(t), y_{n_A} = A)\}, \quad n_A = 1, 2, \dots, N_A, \\ D_{N_B} &= \{(H_{\varepsilon_0^{n_B}, \varepsilon_u^{n_B}}^B(t), y_{n_B} = B)\}, \quad n_B = N_A + 1, N_A + 2, \dots, N, \end{aligned} \quad (22)$$

where

$$H_{\varepsilon_0^{n_A}, \varepsilon_u^{n_A}}^A(t) = g_0^A(\varepsilon_0^{n_A})H_0 + g_u^A(\varepsilon_u^{n_A}) \sum_{m=1}^M u_m(t)H_m$$

and

$$H_{\varepsilon_0^{n_B}, \varepsilon_u^{n_B}}^B(t) = g_0^B(\varepsilon_0^{n_B})H_0 + g_u^B(\varepsilon_u^{n_B}) \sum_{m=1}^M u_m(t)H_m.$$

Using the training set (22), we can construct a generalized system as follows

$$\frac{d}{dt} \begin{pmatrix} |\psi_{\varepsilon_0^1, \varepsilon_u^1}^A(t)\rangle \\ \vdots \\ |\psi_{\varepsilon_0^{N_A}, \varepsilon_u^{N_A}}^A(t)\rangle \\ |\psi_{\varepsilon_0^{N_A+1}, \varepsilon_u^{N_A+1}}^B(t)\rangle \\ \vdots \\ |\psi_{\varepsilon_0^N, \varepsilon_u^N}^B(t)\rangle \end{pmatrix} = -i \begin{pmatrix} H_{\varepsilon_0^1, \varepsilon_u^1}^A(t) |\psi_{\varepsilon_0^1, \varepsilon_u^1}^A(t)\rangle \\ \vdots \\ H_{\varepsilon_0^{N_A}, \varepsilon_u^{N_A}}^A(t) |\psi_{\varepsilon_0^{N_A}, \varepsilon_u^{N_A}}^A(t)\rangle \\ H_{\varepsilon_0^{N_A+1}, \varepsilon_u^{N_A+1}}^B(t) |\psi_{\varepsilon_0^{N_A+1}, \varepsilon_u^{N_A+1}}^B(t)\rangle \\ \vdots \\ H_{\varepsilon_0^N, \varepsilon_u^N}^B(t) |\psi_{\varepsilon_0^N, \varepsilon_u^N}^B(t)\rangle \end{pmatrix}. \quad (23)$$

The performance function for this generalized system is defined by

$$J_N(u) := w_A J^A + w_B J^B, \quad (24)$$

where

$$\begin{aligned} J^A &= \frac{1}{N_A} \sum_{n_A=1}^{N_A} J_{\varepsilon_0^{n_A}, \varepsilon_u^{n_A}}^A(u) = \frac{1}{N_A} \sum_{n_A=1}^{N_A} |\langle \psi_{\varepsilon_0^{n_A}, \varepsilon_u^{n_A}}^A(T) | \psi_{\text{targetA}} \rangle|^2, \\ J^B &= \frac{1}{N_B} \sum_{n_B=N_A+1}^N J_{\varepsilon_0^{n_B}, \varepsilon_u^{n_B}}^B(u) = \frac{1}{N_B} \sum_{n_B=N_A+1}^N |\langle \psi_{\varepsilon_0^{n_B}, \varepsilon_u^{n_B}}^B(T) | \psi_{\text{targetB}} \rangle|^2. \end{aligned} \quad (25)$$

The task of the training step is to find a control strategy that maximizes the performance function defined in (24). From equations (16), (24) and (25), we have

$$\begin{aligned} \nabla J_N(u_m^k) &= \frac{2w_a}{N_A} \sum_{n_A=1}^{N_A} \Im \left(\langle \psi_{\varepsilon_0^{n_A}, \varepsilon_u^{n_A}}^A(T) | \psi_{\text{targetA}} \rangle \langle \psi_{\text{targetA}} | G_{n_A, m}^A(t) | \psi_0 \rangle \right) \\ &\quad + \frac{2w_b}{N_B} \sum_{n_B=N_A+1}^N \Im \left(\langle \psi_{\varepsilon_0^{n_B}, \varepsilon_u^{n_B}}^B(T) | \psi_{\text{targetB}} \rangle \langle \psi_{\text{targetB}} | G_{n_B, m}^B(t) | \psi_0 \rangle \right) \end{aligned} \quad (26)$$

where

$$\begin{aligned} G_{n_A, m}^A(t) &= U_{\varepsilon_0^{n_A}, \varepsilon_u^{n_A}}^A(T) U_{\varepsilon_0^{n_A}, \varepsilon_u^{n_A}}^{\dagger}(t) g_u^A(\varepsilon_u^{n_A}) H_m U_{\varepsilon_0^{n_A}, \varepsilon_u^{n_A}}^A(t), \\ G_{n_B, m}^B(t) &= U_{\varepsilon_0^{n_B}, \varepsilon_u^{n_B}}^B(T) U_{\varepsilon_0^{n_B}, \varepsilon_u^{n_B}}^{\dagger}(t) g_u^B(\varepsilon_u^{n_B}) H_m U_{\varepsilon_0^{n_B}, \varepsilon_u^{n_B}}^B(t). \end{aligned}$$

Then we design the SLC algorithm (*Algorithm 2*) for binary QEC using the gradient flow method to approximate an optimal control strategy $u^* = \{u_m^*(t)\}$.

Remark 2: Both *Algorithm 1* and *Algorithm 2* are developed using the gradient flow method. Their convergence is closely related to quantum control problems. According to the theory of quantum control landscape [33], [34], gradient-based algorithms are effective for trap-free quantum optimal control problems and many practical quantum control problems are trap-free problems [35]-[36]. The classification considered in this paper is trap-free. For those complex quantum control problems (e.g., control of multi-level open quantum systems), stochastic learning techniques (e.g., genetic algorithms) may be required.

Remark 3: As for the specific techniques of choosing samples (N members of the ensemble), we generally choose them according to the functions $g_0^A(\cdot)$, $g_u^A(\cdot)$, $g_0^B(\cdot)$ and $g_u^B(\cdot)$, and the distribution of the inhomogeneity parameters ε_0 and ε_u . It is clear that the basic motivation of the proposed sampling-based learning control approach is to design a control law using only a few sampling members instead of the whole ensemble (consisting of a large number of members). Therefore, it is necessary to choose the samples that are representative for the quantum ensemble. Generally if we know the distribution of the parameter dispersion, it is practical and convenient to choose artificial members for the construction of the generalized system. In numerical examples,

Algorithm 2. SLC for binary QEC

- 1: Set the index of iterations $k = 0$
- 2: Choose a set of arbitrary controls $u^{k=0}(t) = \{u_m^0(t), m = 1, 2, \dots, M\}, t \in [0, T]$
- 3: **repeat** (for each iterative process)
- 4: **repeat** (for each member in training subset D_{N_A} , $n_A = 1, 2, \dots, N_A$)
- 5: Compute the propagator $U_{\varepsilon_0^{n_A}, \varepsilon_u^{n_A}}^k(t)$ with the control strategy $u^k(t)$
- 6: **until** $n_A = N_A$
- 7: **repeat** (for each member in training subset D_{N_B} , $n_B = N_A + 1, N_A + 2, \dots, N$)
- 8: Compute the propagator $U_{\varepsilon_0^{n_B}, \varepsilon_u^{n_B}}^k(t)$ with the control strategy $u^k(t)$
- 9: **until** $n_B = N$
- 10: **repeat** (for each control $u_m(t)$ ($m = 1, 2, \dots, M$) of the control vector $u^k(t)$)
- 11: $\delta_m^k(t) := \nabla J_N(u_m^k)$ and compute $\nabla J_N(u_m^k)$ using equation (26)
- 12: $u_m^{k+1}(t) = u_m^k(t) + \eta_k \delta_m^k(t)$
- 13: **until** $m = M$
- 14: $k = k + 1$
- 15: **until** the learning process ends
- 16: The optimal control strategy $u^*(t) = \{u_m^*(t)\} = \{u_m^k(t)\}, m = 1, 2, \dots, M$

we will demonstrate the detailed method for choosing samples and more related topics have also been discussed in [27], [31]. In addition, overlapped distributions of the inhomogeneity parameters for class A and class B may lead to the problem of overlapped classification, which is a challenging task even for classical classification problems [37]. In the next subsection, we demonstrate the classification performance for both cases with and without class overlapping.

B. Numerical examples

We consider two-level quantum systems. For two similar classes of members in an inhomogeneous quantum ensemble, the Hamiltonians can be described as

$$\begin{aligned} H_{\varepsilon_0, \varepsilon_u}^A(t) &= \frac{1}{2}g_0^A(\varepsilon_0)\sigma_z + \frac{1}{2}g_u^A(\varepsilon_u)(u_1(t)\sigma_x + u_2(t)\sigma_y), \\ H_{\varepsilon_0, \varepsilon_u}^B(t) &= \frac{1}{2}g_0^B(\varepsilon_0)\sigma_z + \frac{1}{2}g_u^B(\varepsilon_u)(u_1(t)\sigma_x + u_2(t)\sigma_y). \end{aligned} \quad (27)$$

Assume $g_0^A(\varepsilon_0) = \varepsilon_0$ with distribution $d_0^A(\varepsilon_0)$, $g_u^A(\varepsilon_u) = \varepsilon_u$ with distribution $d_u^A(\varepsilon_u)$, $g_0^B(\varepsilon_0) = \varepsilon_0$ with distribution $d_0^B(\varepsilon_0)$, and $g_u^B(\varepsilon_u) = \varepsilon_u$ with distribution $d_u^B(\varepsilon_u)$.

Suppose the distributions of ε_0 and ε_u for class A are $d_0^A(\varepsilon_0) = \Phi(\frac{\varepsilon_0 - \mu_0^A}{\sigma_0^A})$ and $d_u^A(\varepsilon_u) = \Phi(\frac{\varepsilon_u - \mu_u^A}{\sigma_u^A})$, respectively, where $\Phi(x) = \int_{-\infty}^x \frac{1}{\sqrt{2\pi}} \exp(-\frac{1}{2}v^2) dv$ is the distribution function of the standard normal distribution. We may choose some equally spaced samples in the $\varepsilon_0 - \varepsilon_u$ space. For example, we may choose the intervals of $[\mu_0^A - 3\sigma_0^A, \mu_0^A + 3\sigma_0^A]$ and $[\mu_u^A - 3\sigma_u^A, \mu_u^A + 3\sigma_u^A]$, and divide them into $N_{\varepsilon_0}^A + 1$ and $N_{\varepsilon_u}^A + 1$ subintervals, respectively, where $N_{\varepsilon_0}^A$ and $N_{\varepsilon_u}^A$ are usually positive odd numbers. Then the number of samples for class A is $N_A = N_{\varepsilon_0}^A N_{\varepsilon_u}^A$, where $\varepsilon_0^{n_A}$ and $\varepsilon_u^{n_A}$ can be chosen from the combination of $(\varepsilon_0^{n_A}, \varepsilon_u^{n_A})$ as follows

$$\begin{cases} \varepsilon_0^{n_A} \in \{\varepsilon_0^{n_A} = \mu_0^A - 3\sigma_0^A + \frac{(2n_A^0 - 1)3\sigma_0^A}{N_{\varepsilon_0}^A}, n_A^0 = 1, 2, \dots, N_{\varepsilon_0}^A\}, \\ \varepsilon_u^{n_A} \in \{\varepsilon_u^{n_A} = \mu_u^A - 3\sigma_u^A + \frac{(2n_A^u - 1)3\sigma_u^A}{N_{\varepsilon_u}^A}, n_A^u = 1, 2, \dots, N_{\varepsilon_u}^A\}. \end{cases} \quad (28)$$

In practical applications, the numbers of $N_{\varepsilon_0}^A$ and $N_{\varepsilon_u}^A$ can be chosen by experience or be tried through numerical computation. As long as the generalized system can model the quantum ensemble and is effective to find the optimal control strategy, we prefer smaller numbers $N_{\varepsilon_0}^A$ and $N_{\varepsilon_u}^A$ to speed up the training process and simplify the generalized system. A similar expression to (28) defines the samples for class B . We use the performance function as defined in (24) with $w_A = w_B = 0.5$. Now we use *Algorithm 2* to find the optimal control strategy.

The parameter settings are listed as follows: $w_A = w_B = 0.5$, the initial state for each member of the quantum ensemble $C_0 = (1, 0)^T$, i.e., $|\psi_0\rangle = |0\rangle$, and the target state for members belonging to class A $C_{\text{targetA}} = (1, 0)^T$, i.e., $|\psi_{\text{targetA}}\rangle = |0\rangle$; the target state for elements belonging to class B $C_{\text{targetB}} = (0, 1)^T$, i.e., $|\psi_{\text{targetB}}\rangle = |1\rangle$; The ending time $T = 8$ (in atomic units) and the total time duration $[0, T]$ is equally discretized into $Q = 800$ time slices with each time slice $\Delta t = (t_q - t_{q-1})|_{q=1,2,\dots,Q} = T/Q = 0.01$; $N_{\varepsilon_0}^A = N_{\varepsilon_u}^A = N_{\varepsilon_0}^B = N_{\varepsilon_u}^B = 5$; the learning rate $\eta_k = 0.2$; the control strategy is initialized as $u^{k=0}(t) = \{u_1^0(t) = \sin t, u_2^0(t) = \sin t\}$.

In the training step, we use $J(u)$ as the performance function which represents the measure of weighted accuracy for QEC. After we apply the optimized control u^* to the inhomogeneous quantum ensemble, we use fidelity to characterize how well every member is classified. The fidelity between the final state $|\psi_{\varepsilon_0, \varepsilon_u}^A(T)\rangle$ of a member belonging to class A and the target state

$|\psi_{\text{targetA}}\rangle$ is defined as follows [4]

$$F(|\psi_{\varepsilon_0, \varepsilon_u}^A(T)\rangle, |\psi_{\text{targetA}}\rangle) = |\langle \psi_{\varepsilon_0, \varepsilon_u}^A(T) | \psi_{\text{targetA}} \rangle|. \quad (29)$$

A similar representation can be defined for the final state $|\psi_{\varepsilon_0, \varepsilon_u}^B(T)\rangle$ of a member belonging to class B and the target state $|\psi_{\text{targetB}}\rangle$. It is clear that the accuracy of QEC can be calculated with

$$\begin{aligned} \zeta &= J(u) = \frac{1}{2}(\mathbb{E}[J^A] + \mathbb{E}[J^B]) \\ &= \frac{1}{2}(\mathbb{E}[F^2(|\psi_{\varepsilon_0, \varepsilon_u}^A(T)\rangle, |\psi_{\text{targetA}}\rangle)] \\ &\quad + \mathbb{E}[F^2(|\psi_{\varepsilon_0, \varepsilon_u}^B(T)\rangle, |\psi_{\text{targetB}}\rangle)]). \end{aligned} \quad (30)$$

We demonstrate and analyze several groups of numerical examples for the cases (1), (2) and (3) with class overlapping, whose parameters characterizing the inhomogeneity are listed as in Table I.

Distribution Function	$d_0^A(\varepsilon_0) = \Phi(\frac{\varepsilon_0 - \mu_0^A}{\sigma_0^A})$	$d_u^A(\varepsilon_u) = \Phi(\frac{\varepsilon_u - \mu_u^A}{\sigma_u^A})$	$d_0^B(\varepsilon_0) = \Phi(\frac{\varepsilon_0 - \mu_0^B}{\sigma_0^B})$	$d_u^B(\varepsilon_u) = \Phi(\frac{\varepsilon_u - \mu_u^B}{\sigma_u^B})$
	$(\mu_0^A, 3\sigma_0^A)$	$(\mu_u^A, 3\sigma_u^A)$	$(\mu_0^B, 3\sigma_0^B)$	$(\mu_u^B, 3\sigma_u^B)$
case (1)	(0.85,0.05)	(0.85,0.05)	(1.15,0.05)	(1.15,0.05)
case (2)	(0.85,0.15)	(0.85,0.15)	(1.15,0.15)	(1.15,0.15)
case (3)	(0.80,0.05)	(0.80,0.05)	(1.20,0.05)	(1.20,0.05)

TABLE I
THE PARAMETERS CHARACTERIZING THE INHOMOGENEITY DISTRIBUTION.

The learning control performance for *case (1)* is shown in Fig. 8 and Fig. 9. As shown in Fig. 8, the learning algorithm converges quickly after about 8000 steps of iterations and finds an optimized control for the coherent control step of binary QEC. Applying the learned control to 300 randomly selected testing samples (150 for *class A* and 150 for *class B*), the control performance is shown in Fig. 9. The mean value of fidelity for the testing of *class A* is 0.9976 and for *class B* is 0.9985. With additional 10^4 testing samples for both *class A* and *class B*, the classification accuracy in *case (1)* is estimated as $\zeta = 99.62\%$.

Compared with *case (1)*, we study the effect of larger dispersion on the Hamiltonian in *case (2)* with larger deviation. The learning control performance for *case (2)* is shown in Fig. 10

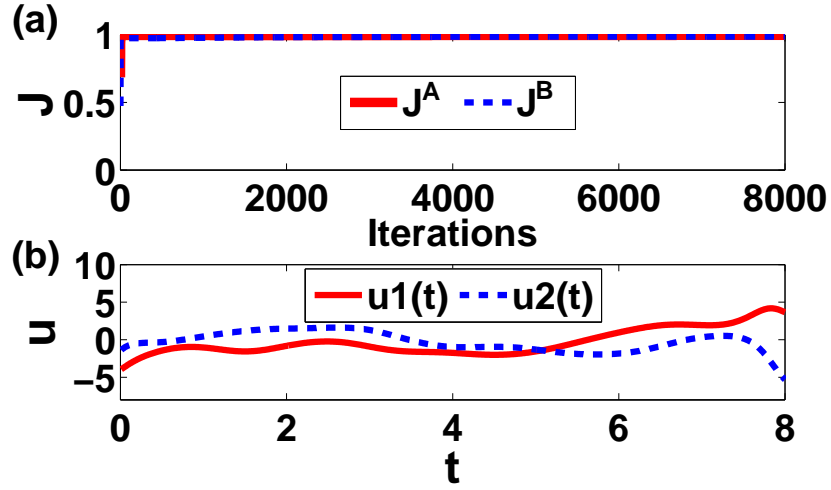


Fig. 8. Learning performance of binary QEC for case (1): (a) evolution of performance function J^A and J^B ; (b) the learned optimal control for QEC.

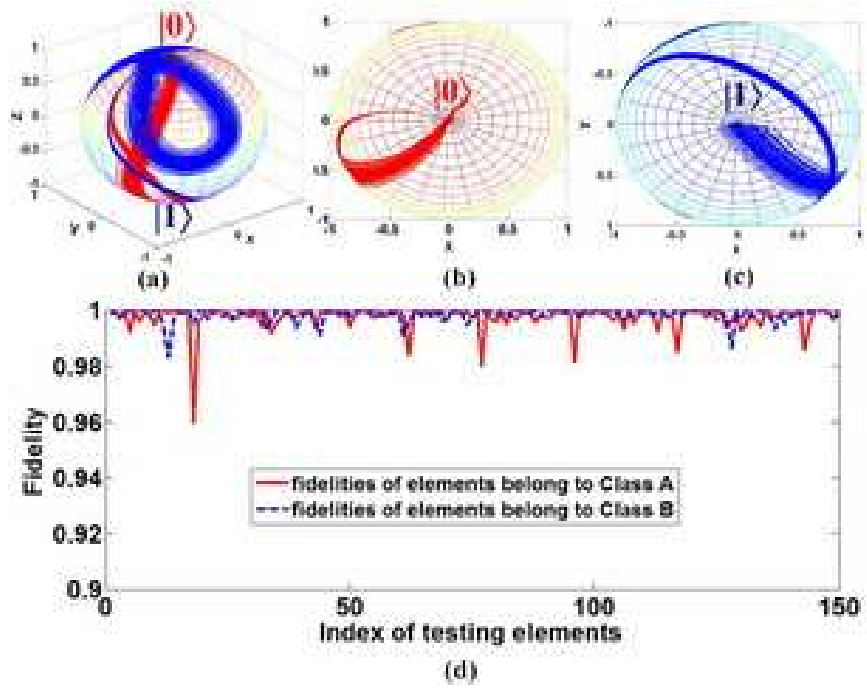


Fig. 9. Control performance of binary QEC for case (1): (a) demonstration of the state transition of all members on the Bloch sphere using the same learned control; (b) trajectories of state transition for members in class A from $|\psi_0\rangle = |0\rangle$ to $|\psi_{\text{targetA}}\rangle = |0\rangle$; (c) trajectories of state transition for members in class B from $|\psi_0\rangle = |0\rangle$ to $|\psi_{\text{targetB}}\rangle = |1\rangle$; (d) control performance regarding fidelity.

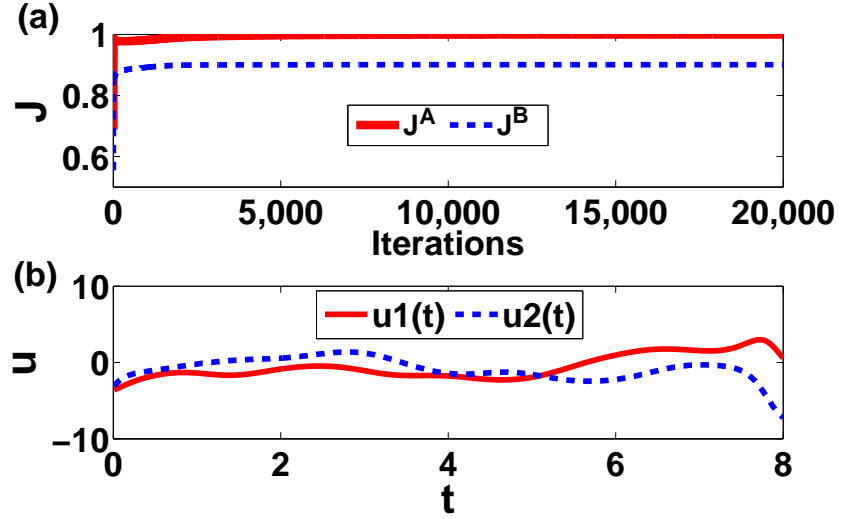


Fig. 10. Learning performance of binary QEC in *case (2)*: (a) evolution of performance function J^A and J^B ; (b) the learned optimal control for QEC.

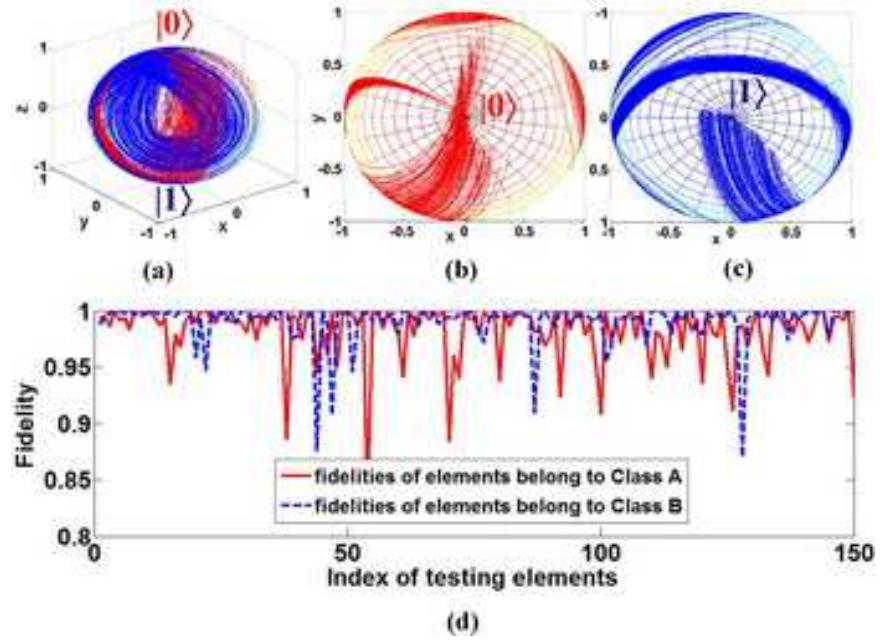


Fig. 11. Control performance of binary QEC for *case (2)*: (a) demonstration of the state transition of all members on the Bloch sphere using the same learned control; (b) trajectories of state transition for members in *class A* from $|\psi_0\rangle = |0\rangle$ to $|\psi_{\text{targetA}}\rangle = |0\rangle$; (c) trajectories of state transition for members in *class B* from $|\psi_0\rangle = |0\rangle$ to $|\psi_{\text{targetB}}\rangle = |1\rangle$; (d) control performance regarding fidelity.

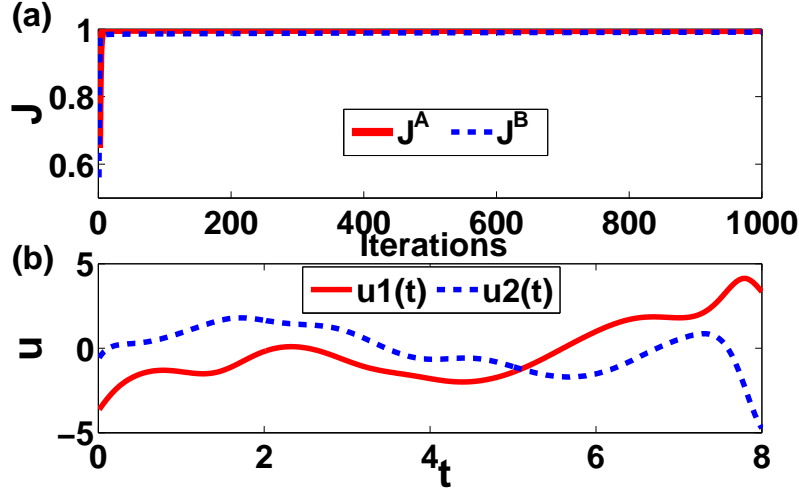


Fig. 12. Learning performance of binary QEC in *case (3)*: (a) evolution of performance function J^A and J^B ; (b) the learned optimal control for QEC.

and Fig. 11. As shown in Fig. 10(a), many more learning steps are needed to find a satisfactory control and the learned optimal control is shown in Fig. 10(b). Due to a larger dispersion, the control performance is a little worse than that in *case (1)*. The mean value of fidelity for the testing of *class A* is 0.9821 and for *class B* is 0.9905. With an additional 10^4 testing samples for both *class A* and *class B*, the classification accuracy in *case (2)* is estimated as $\zeta = 97.35\%$.

In *case (3)*, we further study the effect of a larger difference of Hamiltonian between *class A* and *class B*. The difference between the means of the distribution in *case (1)* $|\mu_0^A - \mu_0^B| = 0.3$ and $|\mu_u^A - \mu_u^B| = 0.3$, while in *case (3)* $|\mu_0^A - \mu_0^B| = 0.4$ and $|\mu_u^A - \mu_u^B| = 0.4$. The learning control performance for *case (3)* is shown in Fig. 12 and Fig. 13. As shown in Fig. 12(a), much fewer learning steps are needed to find a satisfactory control and the learned optimal control is shown in Fig. 12(b). Due to larger difference between *class A* and *class B*, the control performance is better than that in *case (1)*. The mean value of fidelity for testing of *class A* is 0.9992 and for *class B* is 0.9996. With additional 10^4 testing samples for both *class A* and *class B*, the classification accuracy in *case (3)* is estimated as $\zeta = 99.88\%$.

From the numerical results in the above three cases, we have the following conclusions: first, the SLC approach is effective for the binary QEC problem and can achieve a high level of classification accuracy; second, the classification performance is deteriorated with larger dispersion on the Hamiltonian and smaller difference of Hamiltonians between *class A* and *class B*.

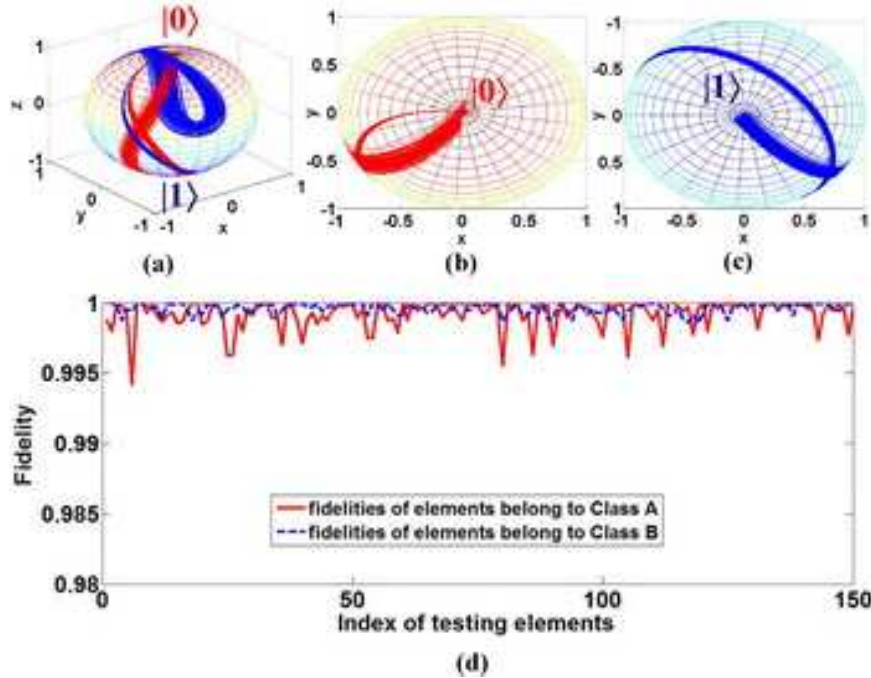


Fig. 13. Control performance of binary QEC in *case (3)*: (a) demonstration of the state transition of all members on the Bloch sphere using the same learned control; (b) trajectories of state transition for members in *class A* from $|\psi_0\rangle = |0\rangle$ to $|\psi_{\text{targetA}}\rangle = |0\rangle$; (c) trajectories of state transition for members in *class B* from $|\psi_0\rangle = |0\rangle$ to $|\psi_{\text{targetB}}\rangle = |1\rangle$; (d) control performance regarding fidelity.

B. More numerical experiments are carried out and similar findings are obtained. For ease of demonstration, we may use the same deviation σ for all the distributions in a certain case. Define the dispersion on the Hamiltonian as $\text{Disp} = 3\sigma$ and define the difference of the Hamiltonian between class *A* and class *B* as $\text{Diff} = \frac{1}{2}(|\mu_0^A - \mu_0^B| + |\mu_u^A - \mu_u^B|)$. The collective results are shown in Fig. 14 with a 3D Pareto front. For a detailed discussion about Pareto front, please refer to [2].

Remark 4: In this paper, the classification problem under consideration involves class overlapping, which is more challenging than that without class overlapping. The proposed approach can be easily applied to the QEC problem without class overlapping and can obtain even better performance. For example, in *case (1)* its counterpart without class overlapping can be characterized with truncated normal distribution. Let the probability density function of a truncated normal distribution be

$$p(x, \mu, \sigma, l, r) = \frac{\frac{1}{\sigma} \phi\left(\frac{x-\mu}{\sigma}\right)}{\Phi\left(\frac{r-\mu}{\sigma}\right) - \Phi\left(\frac{l-\mu}{\sigma}\right)}$$

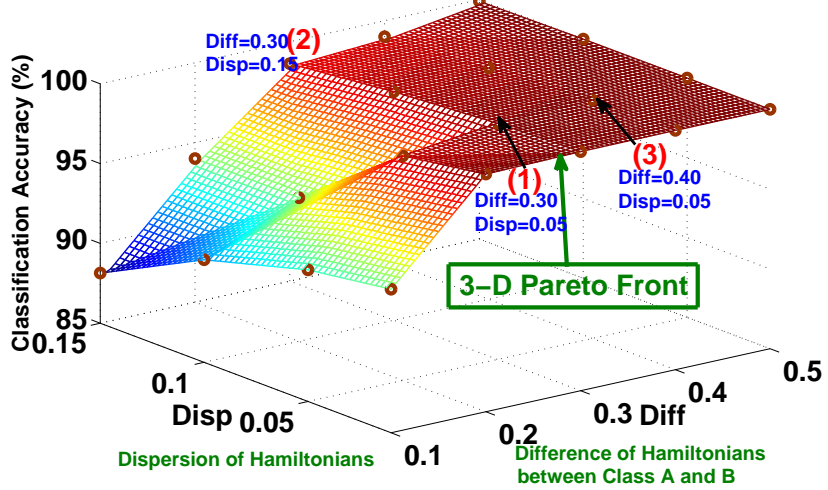


Fig. 14. Three-dimensional Pareto front of binary QEC.

where $\phi(x)$ is the probability density function of the standard normal distribution. The probability density functions for the truncated normal distributions are set as follows:

$$p_0^A = p(\varepsilon_0, \mu_0^A, \sigma_0^A, -\infty, \bar{\mu}_0), \quad p_u^A = p(\varepsilon_u, \mu_u^A, \sigma_u^A, -\infty, \bar{\mu}_u),$$

$$p_0^B = p(\varepsilon_0, \mu_0^B, \sigma_0^B, \bar{\mu}_0, +\infty), \quad p_u^B = p(\varepsilon_u, \mu_u^B, \sigma_u^B, \bar{\mu}_u, +\infty).$$

where $\bar{\mu}_0 = \frac{\mu_0^A + \mu_0^B}{2}$ and $\bar{\mu}_u = \frac{\mu_u^A + \mu_u^B}{2}$. Using the same approach and parameter settings in *case (1)*, we can achieve the classification accuracy $\zeta' = 99.66\%$. Similar comparison is investigated in *case (2)* and *case (3)*. These results are presented in Table II.

case	accuracy ζ with class overlapping	accuracy ζ' without class overlapping
case (1)	$\zeta = 99.62\%$	$\zeta' = 99.66\%$
case (2)	$\zeta = 97.35\%$	$\zeta' = 97.70\%$
case (3)	$\zeta = 99.88\%$	$\zeta' = 99.92\%$

TABLE II

A COMPARISON BETWEEN THE CLASSIFICATION ACCURACY ζ WITH CLASS OVERLAPPING AND THE CLASSIFICATION ACCURACY ζ' WITHOUT CLASS OVERLAPPING FOR DIFFERENT CASES.

V. MULTICLASS CLASSIFICATION OF MULTI-LEVEL QUANTUM ENSEMBLES

In machine learning, multiclass classification involves classifying instances into more than two classes. Some classification algorithms naturally permit the use of more than two classes [38]. A useful strategy is the one-vs-all strategy, where a single classifier is trained per class to distinguish that class from all other classes [39].

The SLC based QEC approach proposed for QEC in Section IV can be extended to multiclass classification of multilevel quantum ensembles using the one-vs-all strategy. For example, an inhomogeneous quantum ensemble consists of three classes of members (i.e., classes A , B and C). First, by applying the binary QEC approach introduced in Section IV, we can classify them into two classes (one for members belonging to class A and the other for all the members belonging to classes B and C). Then we use the binary QEC approach again to classify the members belonging to class B from the members belonging to class C . According to the numerical results demonstrated in Section IV, good classification performance is also expected for these multiclass classification problems. However, the one-vs-all strategy may cause additional cost since the process involves multiple times of binary classification and multiple learning control procedures.

In this section we use a different strategy from the one-vs-all strategy to extend the proposed SLC based classification method to multiclass classification of multi-level quantum ensembles. In this strategy, only one time of quantum coherent control procedure is needed to implement the multiclass QEC.

We consider an inhomogeneous quantum ensemble of three-level Λ -type atomic systems [27]. The evolving state $|\psi(t)\rangle$ of the Λ -type system can be expanded in terms of the eigenstates as follows:

$$|\psi(t)\rangle = c_1(t)|1\rangle + c_2(t)|2\rangle + c_3(t)|3\rangle, \quad (31)$$

where $|1\rangle$, $|2\rangle$ and $|3\rangle$ are the basis states of the lower, middle and upper atomic states, respectively, corresponding to the free Hamiltonian

$$H_0 = \begin{pmatrix} 1.5 & 0 & 0 \\ 0 & 1 & 0 \\ 0 & 0 & 0 \end{pmatrix}. \quad (32)$$

Denote $C(t) = (c_1(t), c_2(t), c_3(t))^T$. To control such a three-level system, we use the control Hamiltonian of $H_u = u_1(t)H_1 + u_2(t)H_2$, where

$$H_1 = \begin{pmatrix} 0 & 0 & 0 \\ 0 & 0 & 1 \\ 0 & 1 & 0 \end{pmatrix}, \quad H_2 = \begin{pmatrix} 0 & 0 & 1 \\ 0 & 0 & 0 \\ 1 & 0 & 0 \end{pmatrix}. \quad (33)$$

Similarly, we describe the inhomogeneous three-level quantum ensemble with the Hamiltonian of each member as

$$H_{\varepsilon_0, \varepsilon_u}(t) = \varepsilon_0 H_0 + \varepsilon_u ((u_1(t)H_1 + u_2(t)H_2)). \quad (34)$$

Suppose that the inhomogeneous quantum ensemble consists of three classes of members labeled with classes A , B and C , respectively. For this multiclass QEC problem, we first use the same control field to drive the members belonging to classes A , B and C from an initial state $|\psi_0\rangle$ to three different target eigenstates ($|1\rangle$, $|2\rangle$ and $|3\rangle$), respectively, so that we can classify them with an additional physical operation (e.g., projective measurement).

We can modify *Algorithm 2* into its multiclass version and then apply it to the three-level inhomogeneous quantum ensemble for finding an optimal control strategy $u^*(t) = \{u_m^*(t), m = 1, 2\}$ to maximize the performance function

$$\begin{aligned} J(u) &= \frac{1}{3}(\mathbb{E}[J^A] + \mathbb{E}[J^B] + \mathbb{E}[J^C]) \\ &= \frac{1}{3}(\mathbb{E}[F^2(|\psi_{\varepsilon_0, \varepsilon_u}^A(T)\rangle, |1\rangle)] + \mathbb{E}[F^2(|\psi_{\varepsilon_0, \varepsilon_u}^B(T)\rangle, |2\rangle)] \\ &\quad + \mathbb{E}[F^2(|\psi_{\varepsilon_0, \varepsilon_u}^C(T)\rangle, |3\rangle)]). \end{aligned} \quad (35)$$

The parameter settings are listed as follows: the initial state $C_0 = (\frac{1}{\sqrt{3}}, \frac{1}{\sqrt{3}}, \frac{1}{\sqrt{3}})$; the three target eigenstates for classes A , B and C are $C_{\text{target}A} = (1, 0, 0)$ (i.e., $|1\rangle$), $C_{\text{target}B} = (0, 1, 0)$ (i.e., $|2\rangle$) and $C_{\text{target}C} = (0, 0, 1)$ (i.e., $|3\rangle$), respectively; the ending time $T = 10$ (in atomic unit) and the total time duration $[0, T]$ is equally discretized into $Q = 1000$ time slices; the learning rate is $\eta_k = 0.2$; the control is initialized as $u^0(t) = \{u_1^0(t) = \text{sint}, u_2^0(t) = \text{sint}\}$. The parameters ε_0 and ε_u characterize the inhomogeneity of the quantum ensemble and they have different normal distributions that are described with the distribution functions $d_0(\varepsilon_0) = \Phi(\frac{\varepsilon_0 - \mu_0}{\sigma_0})$ and $d_u(\varepsilon_u) = \Phi(\frac{\varepsilon_u - \mu_u}{\sigma_u})$, where for class A ($\mu_0^A = 1, 3\sigma_0^A = 0.05$) and ($\mu_u^A = 0.8, 3\sigma_u^A = 0.05$), for class B ($\mu_0^B = 0.8, 3\sigma_0^B = 0.05$) and ($\mu_u^B = 1, 3\sigma_u^B = 0.05$), for class C ($\mu_0^C = 1.2, 3\sigma_0^C = 0.05$) and ($\mu_u^C = 1.2, 3\sigma_u^C = 0.05$). To construct the generalized system for learning the optimal control,

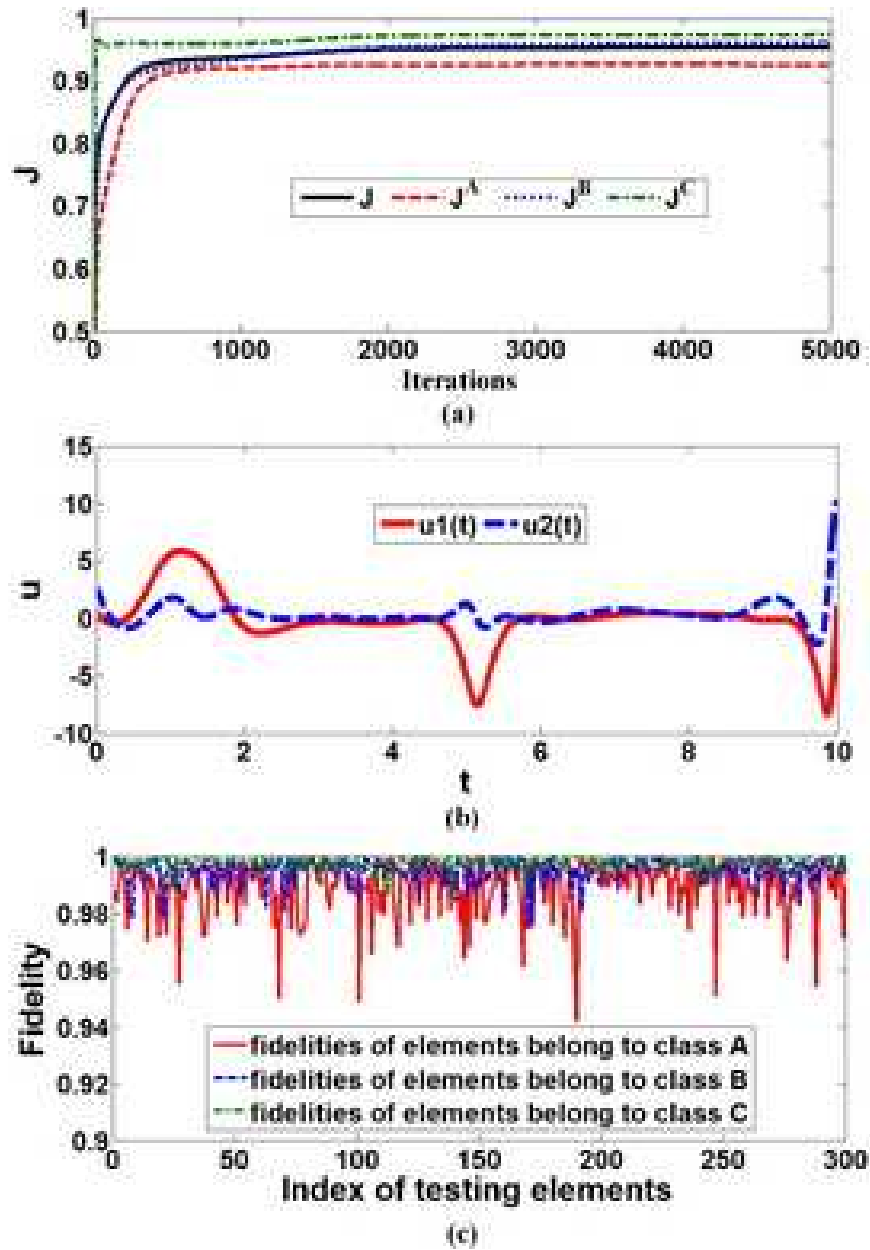


Fig. 15. Learning control performance for multiclass QEC: (a) evolution of performance function $J(u)$ with its three component values $J^A(u)$, $J^B(u)$ and $J^C(u)$; (b) the learned optimal control for the multiclass QEC problem; (c) control performance regarding fidelity.

the sampling method as described in (28) is adopted with setting $N_{\varepsilon_0}^A = N_{\varepsilon_u}^A = N_{\varepsilon_0}^B = N_{\varepsilon_u}^B = N_{\varepsilon_0}^C = N_{\varepsilon_u}^C = 3$.

The learning performance is shown in Fig. 15. The evolution of the performance function $J(u)$ is shown in Fig. 15(a) with its three component values $J^A(u)$, $J^B(u)$ and $J^C(u)$. The results demonstrate that the SLC based classification method is effective for multiclass QEC of multi-level quantum ensembles and has good scalability. The learned optimized control for the coherent control step of QEC is shown in Fig. 15(b). As shown in Fig. 15(c), 300 randomly selected samples for each class of members are tested and all of them are controlled to their corresponding target eigenstates, respectively, with high fidelity. The mean value of fidelity for testing of *class A* is 0.9897, for *class B* is 0.9953 and for *class C* is 0.9976. With additional 10^4 testing samples for each class, we have the classification accuracy $\zeta = 98.80\%$, which verifies the effectiveness of the proposed SLC based approach for QEC.

VI. CONCLUSIONS

In this paper, we present a systematic classification approach for inhomogeneous quantum ensembles by combining an SLC approach with quantum discrimination. The classification process is accomplished via simultaneously steering members belonging to different classes to different corresponding target states (e.g., eigenstates). A new discrimination method is first presented for quantum systems with similar Hamiltonians. Then an SLC method is proposed for quantum ensemble classification. Numerical experiments are carried out to test the performance of the proposed approach for the binary classification of two-level quantum ensembles and the multiclass classification of three-level Λ -type quantum ensembles. All the numerical results demonstrate the effectiveness of the proposed approach for quantum ensemble classification.

APPENDIX

Recall that $J_{\varepsilon_0^a, \varepsilon_u^a}^a(u) = |\langle \psi_{\varepsilon_0^a, \varepsilon_u^a}^a(T) | \psi_{\text{targetA}} \rangle|^2$ and $|\psi_{\varepsilon_0^a, \varepsilon_u^a}^a(t)\rangle$ satisfies

$$\frac{d}{dt} |\psi_{\varepsilon_0^a, \varepsilon_u^a}^a(t)\rangle = -iH_{\varepsilon_0^a, \varepsilon_u^a}^a(t) |\psi_{\varepsilon_0^a, \varepsilon_u^a}^a(t)\rangle, \quad |\psi_{\varepsilon_0^a, \varepsilon_u^a}^a(0)\rangle = |\psi_0\rangle. \quad (36)$$

For ease of notation, we consider the case where only one control is involved, i.e., $H_{\varepsilon_0^a, \varepsilon_u^a}^a(t) = g_0(\varepsilon_0^a)H_0 + u(t)g_u(\varepsilon_u^a)H_1$. The expression of the gradient of $J_{\varepsilon_0^a, \varepsilon_u^a}^a(u)$ with respect to the control u can be derived by using a first order perturbation.

Let $\delta\psi(t)$ be the modification of $|\psi(t)\rangle$ induced by a perturbation of the control from $u(t)$ to $u(t) + \delta u(t)$. By keeping only the first order terms, we obtain the equation satisfied by $\delta\psi$:

$$\begin{cases} \frac{d}{dt}\delta\psi = -i(g_0(\epsilon_0^a)H_0 + u(t)g_u(\epsilon_u^a)H_1)\delta\psi \\ \quad - i\delta u(t)g_u(\epsilon_u^a)H_1|\psi_{\epsilon_0^a, \epsilon_u^a}^a(t)\rangle, \\ \delta\psi(0) = 0. \end{cases} \quad (37)$$

Let $U_{\epsilon_0^a, \epsilon_u^a}(t)$ be the propagator corresponding to (36). Then, $U_{\epsilon_0^a, \epsilon_u^a}(t)$ satisfies

$$\frac{d}{dt}U_{\epsilon_0^a, \epsilon_u^a}(t) = -iH_{\epsilon_0^a, \epsilon_u^a}^a(t)U_{\epsilon_0^a, \epsilon_u^a}(t), \quad U(0) = I. \quad (38)$$

Therefore,

$$\begin{aligned} \delta\psi(T) &= -iU_{\epsilon_0^a, \epsilon_u^a}(T)\int_0^T \delta u(t)U_{\epsilon_0^a, \epsilon_u^a}^\dagger(t)g_u(\epsilon_u^a)H_1|\psi_{\epsilon_0^a, \epsilon_u^a}^a(t)\rangle dt \\ &= -iU_{\epsilon_0^a, \epsilon_u^a}(T)\int_0^T U_{\epsilon_0^a, \epsilon_u^a}^\dagger(t)g_u(\epsilon_u^a)H_1U_{\epsilon_0^a, \epsilon_u^a}(t)\delta u(t)dt |\psi_0\rangle \end{aligned} \quad (39)$$

where U^\dagger is the adjoint of U . Using (39), we have

$$\begin{aligned} &J_{\epsilon_0^a, \epsilon_u^a}^a(u + \delta u) \\ &\approx J_{\epsilon_0^a, \epsilon_u^a}^a(u) + 2\Re\left(\langle\psi_{\epsilon_0^a, \epsilon_u^a}^a(T)|\psi_{\text{targetA}}\rangle\langle\psi_{\text{targetA}}|\delta\psi(T)\rangle\right) \\ &= J_{\epsilon_0^a, \epsilon_u^a}^a(u) + 2\Re\left(-i\langle\psi_{\epsilon_0^a, \epsilon_u^a}^a(T)|\psi_{\text{targetA}}\rangle\langle\psi_{\text{targetA}}|\int_0^T G_1^a(t)\delta u(t)dt|\psi_0\rangle\right) \\ &= J_{\epsilon_0^a, \epsilon_u^a}^a(u) + \int_0^T 2\Im\left(\langle\psi_{\epsilon_0^a, \epsilon_u^a}^a(T)|\psi_{\text{targetA}}\rangle\langle\psi_{\text{targetA}}|G_1^a(t)|\psi_0\rangle\right)\delta u(t)dt \end{aligned} \quad (40)$$

where $G_1^a(t) = U_{\epsilon_0^a, \epsilon_u^a}(T)U_{\epsilon_0^a, \epsilon_u^a}^\dagger(t)g_u(\epsilon_u^a)H_1U_{\epsilon_0^a, \epsilon_u^a}(t)$, $\Re(\cdot)$ and $\Im(\cdot)$ denote respectively the real and imaginary parts of a complex number.

Recall also that the definition of the gradient implies

$$\begin{aligned} J_{\epsilon_0^a, \epsilon_u^a}^a(u + \delta u) &= J_{\epsilon_0^a, \epsilon_u^a}^a(u) + \langle\nabla J_{\epsilon_0^a, \epsilon_u^a}^a(u), \delta u\rangle_{L^2([0, T])} + o(\|\delta u\|) \\ &= J_{\epsilon_0^a, \epsilon_u^a}^a(u) + \int_0^T \nabla J_{\epsilon_0^a, \epsilon_u^a}^a(u)\delta u(t)dt + o(\|\delta u\|). \end{aligned} \quad (41)$$

Therefore, by identifying (40) with (41), we obtain

$$\nabla J_{\epsilon_0^a, \epsilon_u^a}^a(u) = 2\Im\left(\langle\psi_{\epsilon_0^a, \epsilon_u^a}^a(T)|\psi_{\text{targetA}}\rangle\langle\psi_{\text{targetA}}|G_1^a(t)|\psi_0\rangle\right). \quad (42)$$

REFERENCES

- [1] M. Mohseni, A.M. Steinberg and J.A. Bergou, “Optical realization of optimal unambiguous discrimination for pure and mixed quantum states”, *Physical Review Letters*, Vol. 93, No. 20, p. 200403, 2004.
- [2] V. Beltrani, P. Ghosh and H. Rabitz, “Exploring the capabilities of quantum optimal dynamic discrimination”, *Journal of Chemical Physics*, Vol. 130, p. 164112, 2009.
- [3] M. Guta and W. Kotlowski, “Quantum learning: asymptotically optimal classification of qubit states,” *New Journal of Physics*, Vol. 12, p.123032, 2010.
- [4] M.A. Nielsen and I.L. Chuang, *Quantum Computation and Quantum Information*, Cambridge, England: Cambridge University Press, 2010.
- [5] C. Altafini and F. Ticozzi, “Modeling and control of quantum systems: an introduction,” *IEEE Transactions on Automatic Control*, Vol. 57, No. 8, pp. 1898-1917, 2012.
- [6] D. Dong and I.R. Petersen, “Quantum control theory and applications: A survey,” *IET Control Theory & Applications*, Vol. 4, pp. 2651-2671, 2010.
- [7] C. Chen, D. Dong, H.X. Li, J. Chu and T.J. Tarn, “Fidelity-based probabilistic Q-learning for control of quantum systems”, *IEEE Transactions on Neural Networks and Learning Systems*, in press, 2013.
- [8] B. Qi, Z.B. Hou, L. Li, D. Dong, G.Y. Xiang and G.C. Guo, “Quantum state tomography via linear regression estimation,” *Scientific Reports*, Vol. 3, p.3496.
- [9] H.M. Wiseman and G.J. Milburn, *Quantum Measurement and Control*, Cambridge, England: Cambridge University Press, 2010.
- [10] B. Li, G. Turinici, V. Ramakrishna and H. Rabitz, “Optimal dynamic discrimination of similar molecules through quantum learning control”, *Journal of Physical Chemistry B*, Vol. 106, No. 33, pp.8125-8131, 2002.
- [11] B. Yoshida, “Classification of quantum phases and topology of logical operators in an exactly solved model of quantum codes”, *Annals of Physics*, Vol. 326, pp.15-95, 2011.
- [12] A. Mitra and H. Rabitz, “Mechanistic analysis of optimal dynamic discrimination of similar quantum systems”, *Journal of Physical Chemistry A*, Vol. 108, No. 21, pp.4778-4785, 2004.
- [13] B. Li, H. Rabitz and J.P. Wolf, “Optimal dynamic discrimination of similar quantum systems with time series data”, *Journal of Chemical Physics*, Vol. 122, p.154103, 2005.
- [14] B. Li, W. Zhu and H. Rabitz, “Optimal dynamic discrimination of similar quantum systems in the presence of decoherence”, *Journal of Chemical Physics*, Vol. 124, p.024101, 2006.
- [15] G. Turinici, V. Ramakrishna, B. Li and H. Rabitz, “Optimal discrimination of multiple quantum systems: controllability analysis”, *Journal of Physics A: Mathematical and General*, Vol. 37, pp.273-282, 2004.
- [16] J. Roslund, M. Roth, L. Guyon, V. Boutou, F. Courvoisier, J. Wolf and H. Rabitz, “Resolution of strongly competitive product channels with optimal dynamic discrimination: application to flavins,” *Journal of Chemical Physics*, Vol. 134, p. 034511, 2011.
- [17] J.A. Bergou, U. Herzog and M. Hillery, “Quantum filtering and discrimination between sets of boolean functions”, *Physical Review Letters*, Vol. 90, No. 25, p.257901, 2003.
- [18] R. Duan, Y. Feng and M. Ying, “Entanglement is not necessary for perfect discrimination between unitary operations”, *Physical Review Letters*, Vol. 98, p.100503, 2007.
- [19] A. Rothman, T.S. Ho and H. Rabitz, “Quantum observable homotopy tracking control”, *Journal of Chemical Physics*, Vol. 123, p.134104, 2005.

- [20] A. Rothman, T.S. Ho and H. Rabitz, “Observable-preserving control of quantum dynamics over a family of related systems”, *Physical Review A*, Vol. 72, p.023416, 2005.
- [21] R. Chakrabarti, R. Wu and H. Rabitz, “Quantum Pareto optimal control”, *Physical Review A*, Vol. 78, p.033414, 2008.
- [22] D.G. Cory, A.F. Fahmy and T.F. Havel, “Ensemble quantum computing by NMR spectroscopy,” *Proceedings of the National Academy of Sciences of the United States of America*, 94: 1634-1639, 1997.
- [23] L.M. Duan, M.D. Lukin, J.I. Cirac and P. Zoller, “Long-distance quantum communication with atomic ensembles and linear optics,” *Nature*, 414: 413-418, 2001.
- [24] J.S. Li, J. Ruths, T.Y. Yu, H. Arthanari, G. Wagner, “Optimal pulse design in quantum control: A unified computational method,” *Proceedings of the National Academy of Sciences of the United States of America*, 108: 1879-1884, 2011.
- [25] Levitt M H. Composite pulses. *Progress in NMR Spectroscopy*, 1986, 18: 61-122.
- [26] J.S. Li, N. Khaneja, “Control of inhomogeneous quantum ensembles”, *Physical Review A*, 2006, 73: 030302(R).
- [27] C. Chen, D. Dong, R. Long, I.R. Petersen and H. Rabitz, “Sampling-based learning control of inhomogeneous quantum ensembles”, *arXiv: 1308.1454 [quant-ph]* 7 August 2013.
- [28] D. Brinks, F.D. Stefani, F. Kulzer, R. Hildner, T.H. Taminiau, Y. Avlasevich, K. Müllen and N.F. van Hulst, “Visualizing and controlling vibrational wave packets of single molecules,” *Nature*, Vol. 465, No. 17, pp. 905-908, 2010.
- [29] J. Ruths and J.S. Li, “A multidimensional pseudospectral method for optimal control of quantum ensembles,” *Journal of Chemical Physics*, vol. 134, p.044128, 2011.
- [30] K. Beauchard, P. S. P. da Silva and P. Rouchon, “Stabilization for an ensemble of half-spin systems,” *Automatica*, Vol. 48, pp. 68-76, 2012.
- [31] D. Dong, C. Chen, R. Long, B. Qi, I.R. Petersen, “Sampling-based learning control for quantum systems with Hamiltonian uncertainties,” *Proceedings of the 52th IEEE Conference on Decision and Control*, December 10-13, 2013, Firenze, Italy. <http://arxiv.org/abs/1312.4370>.
- [32] D.M. Appleby, “Optimal measurement of spin direction,” *International Journal of Theoretical Physics*, Vol. 39, No. 9, pp. 2231-2252, 2000.
- [33] H. Rabitz, M. Hsieh and C. Rosenthal “Quantum optimally controlled transition landscapes,” *Science*, vol. 303, pp. 1998-2001, 2004.
- [34] R. Chakrabarti and H. Rabitz, “Quantum control landscapes,” *International Reviews in Physical Chemistry*, vol. 26, no. 4, pp. 671-735, 2007.
- [35] H. Jirari and W. Pötz, “Optimal coherent control of dissipative N-level systems”, *Physical Review A*, Vol. 72, p. 013409, 2005.
- [36] J. Roslund and H. Rabitz, “Gradient algorithm applied to laboratory quantum control”, *Physical Review A*, Vol. 79, p. 053417, 2009.
- [37] C.L. Liu, “Partial discriminative training for classification of overlapping classes in document analysis”, *International Journal on Document Analysis and Recognition*, Vol. 11, pp. 53-65, 2008.
- [38] M. Lin, K. Tang and X. Yao, “Dynamic sampling approach to training neural networks for multiclass imbalance classification”, *IEEE Transactions on Neural Networks and Learning Systems*, Vol. 24, No. 4, pp.647-660, 2013.
- [39] R. Rifkin and A. Klautau, “In defence of one-vs-all classification”, *Journal of Machine Learning Research*, Vol. 5, pp. 101-141, 2004.